UNESCO-IHE
Institute for Water Education

Mountain Risks

MARIE CURIE ACTIONS

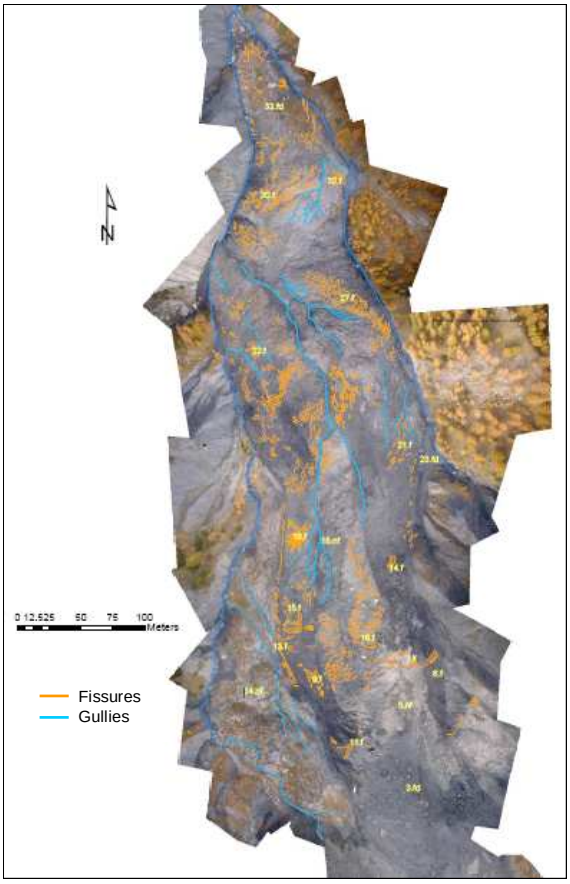

ANALYISIS AND QUANTIFICATION OF PREFERENTIAL FLOW ON THE SUPER SAUZE LANSLIDE

Angela Alexandra Arévalo Espinosa
MSc. Thesis WSE-HWR-09.01
Delft, 2009

UNESCO-IHE
Institute for Water Education

Mountain Risks

MARIE CURIE ACTIONS

ANALYISIS AND QUANTIFICATION OF PREFERENTIAL FLOW ON THE SUPER SAUZE LANSLIDE

Master of Science Thesis
by
Angela Alexandra Arévalo Espinosa

Supervisor
Prof. Dr. S. Uhlenbrook, PhD, MSc (UNESCO-IHE)

Mentor
Dr. Thom Bogaard (TU DELFT, UNESCO-IHE)

Examination committee
Prof. Dr. S. Uhlenbrook, PhD, MSc (UNESCO-IHE)
Prof. Th. W.J. van Asch (Utrecht University)
T.A. Bogaard, PhD (TU DELFT, UNESCO-IHE)

This research is done for the partial fulfillment of requirements for the Master of Science degree at the UNESCO-IHE Institute for Water Education, Delft, the Netherlands

Delft, May 2009

ABSTRACT

The Super Sauze landslide is one test site of the Mountain Risks project, a Marie Curie Research Training Network. This slow moving landslide has been monitored, with the purpose of understanding the hydrogeological processes involved in the generation of instability. Some studies have highlighted the importance of preferential flows through surface fissures on the fast groundwater recharge.

The methodology followed included four main sections (i) the geomorphological characterization of the landslide including the description of tension-induce fissures, (ii) the assessment of the saturated hydraulic conductivity in the soil matrix and in the material filling the fissures and the occurrence of preferential flow, (iii) the analysis of preferential flow on three sprinkled experiments and (iv) the identification of areas with similar hydrological response.

Large variability of the saturated hydraulic conductivity was found in the matrix and in the fissures, both ranging on four orders of magnitude. However, the mean value of this parameter from the fissures was higher than the values from the soil matrixes. In addition, higher probability of preferential flow was found to occur in the fissures. Probability density functions were defined for both sets of data.

The results of three sprinkler experiments were assessed by using water balances and drawdown curves. Very different hydrological behaviour was identified on the three test locations related including variable infiltration capacity, times of drainage and proportion of preferential and matrix flows. Moreover, it was found that the hydrological behaviour has an influence on the instability conditions of the three locations.

Compared with previously establish modeling areas, it was found that one of them must be split to differentiate a site which feature distinctly higher infiltration capacity than the surrounding places. This area is located in the upper part of the landslide and comprises various types of movements occurring in combination and in small extensions. The high infiltration capacity of the area can play an important role in the groundwater recharge toward downslope sites.

Key words: preferential flow, landslides, hillslope hydrology, Super_Sauze landslide

To the almighty God from whom all good things come,
to my mother and to you.

ACKNOWLEDGMENTS

I am very grateful to my mentor Dr. Thom Bogaard, for his continuous support and valuable suggestions, as well as for his encouragement to face each stage of the research which was fundamental to successfully accomplish it. I also thank him for all his work on the critical reading of preliminary versions and for his dedication to solve all my queries.

I also want to thank Professor Stefan Uhlenbrook for his advice and suggestions for the thesis and also for his motivating professional example.

In addition, I would like to thank Professor Theo van Asch for agreeing to be on my evaluation committee despite his busy schedule.

Thanks also to the professionals of the mountain risk people and to Vincent Knoops for his cooperation during the field work.

I am grateful to the Government of the Netherlands for its funding through a scholarship awarded by Nuffic; to the Mountain Risk project for the funding of the field work activities and to the Delft University of Technology for hosting me during the writing of the thesis.

Finally, I want to express lot of gratitude to all my friends and colleagues for his technical advice or their supportive words. Special thanks to A. Gonzales, D. Krzeminska, J-A Bouchard, F. Gomez and C. Castañeda.

Muchas gracias a todos.

Alexandra Arévalo Espinosa
May 2009

CONTENT

FIGURES

TABLES

1. INTRODUCTION

1.1. BACKGROUND

Risk assessment, which comprises hazard and vulnerability assessment, is considered a key aspect in the risk management field. Many advances in the quantification of risks have taken place in the last decade (Van Westen et al., 2005). In particular, many methods related with landslide hazard assessment have been developed. However, the particularity of the types of landslides and the local characteristics, as well as the complexity of the hydrogeological and geotechnical processes involved, make this field a continual source of questions to be solved.

An integrated approach to risk assessment and management pertaining to mountain hazards is given in the Mountain Risks project, a Marie Curie Research Training Network, which was formulated in the 6th Framework Program of the European Commission. This network intends to develop an advanced understanding of hydro-geomorphological processes in mountainous areas and to apply this understanding to living with the hazards in the long-term.

One of the test sites for the Mountain Risks project is the Super Sauze landslide, which is representative of the reworked landscapes in the Barcelonette Valley, located in southeastern France. This slow moving landslide has been monitored since 1991, with the purpose of understanding the hydrogeological processes involved in the generation of instability. Research from different disciplines such as geotechnics, hydrology, hydrochemistry and geophysics, have led to a better understanding of the processes governing the landslide motion (Montety et al., 2007).

In the Super Sauze landslide, some studies have highlighted the importance of preferential flows through surface fissures on the groundwater recharge. In addition, it has been recognized that the study of the interactions between saturated and non-saturated flows as well as the influence of macropores and fissures are fundamental to understanding the hydrogeological characteristics of the landslide (Malet et al. 2005).

At present, the analysis and quantification of preferential flow on the dynamic behaviour of the landslide is the theme of a doctorate thesis in the Delft University of Technology, done in the frame of the Mountain risks Marie-Curie research and training network.

1.2. PROBLEM DESCRIPTION

In the Super Sauze landslide, precipitation has been determined to be the main source of rapid water table rise which contributes to the increase of instability conditions. Special attention is required for the analysis of preferential flows through tension-induced fissures that exist on the landslide. These fissures comprise open spaces at the soil surface and disturbed soil material underneath. Differences of flow through these fissures and the matrix need to be evaluated.

Additionally, it is expected a spatial difference of the hydraulic characteristics on both domains due the heterogeneity of soil materials in Super Sauze. Although the soil material mostly comprises black marls, the heterogeneity results from different levels of weathering of the soil particles as well as their continuous movement.

A simulation of the hydrological behaviour of the landslide has been performed with a physically based spatially distributed model which incorporated unsaturated and saturated conditions. This model represented well the drainage and the range of groundwater levels but failed in the simulation of the times for recharge. Some rapid recharge events, i.e. less than one day, were modeled as if they last many days. The need of more detailed spatial representation of hydraulic conductivity, porosity and the density of fissures was identified in order to improve the understanding of the recharge from precipitation. The preferential flow throughout the fissures was identified as the main factor contributing to different infiltration rates within the landslide (Malet, et al 2005).

1.3. RESEARCH OBJECTIVES

The main objective of this research is to analyze and quantify the preferential flow within different geomorphologic units in the Super Sauze landslide.

To achieve this, four specific objectives are derived. First, to perform a geomorphological characterization of the landslide. Second, to assess the saturated hydraulic conductivity and the occurrence of preferential flow on different geomorphological units. Third, to analyze preferential flow form three sprinkled experiments done in the landslide site. Finally, to identify areas with similar hydrological response based on relations of the hydrological parameters with the geomorphological descriptors and to the existence of fissures, their size and connectivity.

2. LITERATURE REVIEW

2.1. INFLUENCE OF WATER PRESSURE ON INSTABILITY OF LANDSLIDES

Two main types of mechanisms are identified to the initiation of landslides: one type generates a decrease in shear strength and the other causes an increase in shear stress. Causes of decrease in shear strength include the enhancement of pore water pressure and the decrease of material strength (Bogaard, 2001).

The assessment of the stability of slopes is expressed by the factor of safety, which is the ratio of available shear strength to the sliding forces, in other words, the ratio of the sum of resisting forces to the sum of driving forces. A factor of safety equal to 1 represents a critical stability condition; higher values indicate stability whereas lower values indicate instability. The factor of safety is described with equation 2.1.

$$FS = \frac{C + (\sigma - u)\tan\phi}{\gamma \times w \times sin\alpha} \qquad [2.1]$$

Where σ-u represent the total normal stress, ϕ the angle of friction, w the widht of the slope material and α the angle of the slope. μ is the pore water pressure which equals the water height times the unit weigh of water.

Another factor of importance in slope stability is the time of drainage which is affected by the permeability of the soil. In less permeable soils, an increased water table exerts high pressure for long periods, thus increasing its effect on the soil's behavior. Conversely, in highly permeable soils, the excess of pore pressure is released rapidly so that its influence on the stability is usually negligible (Bromhead, 1986).

The increase of water pressure caused by the rise of the groundwater table is of particular interest to this research. This process occurs over short periods in the Super Sauze landslide due to quick infiltration and a shallow groundwater system.

2.2. PREFERENTIAL FLOW ASSESSMENT

According to Kirkby (1978), preferential flow or flow through macropores is that occurring in spaces that are bigger that the capillary-size pores of the soil's

matrix. The preferential flow is turbulent; therefore it is not well described by Darcy principle of flow through porous media (Bevenn & Germann, 1982). Therefore, preferential flow has to be determined by indirect methods.

Bevenn & Germann (1980) also affirm that there is no a unique criteria to differentiate pores of macropores in the micro-scale. Instead, used criteria are arbitrary and mainly defined for experimental purposes. Furthermore, in such criteria would be required to consider that not only the size but the connection between the macropores define if they are hydrologically effective. On the other hand, when describing morphology of the soils, the visible macropores are easily identifiable features. From this point of view the macropores are classified as those formed by soil fauna, those formed by plant roots, cracks and fissures and natural soil pipes.

Kirkby (1978) cites an approach for calculating macropore flow by using equations of open channels or pipes which are derived from the Darcy-Weisbach equation. However, it is stated by the same author that these type of equations are unlikely to be useful because a lack of measurements of required variables of velocities and flow resistance in natural conditions.

Several other studies have been carried out in recent years to describe and to quantify preferential flow. For instance, Weiler (2001) recognize a strong influence of flow through macropores on infiltration as well as in runoff generation. Other authors as Bouma et al., (1982) and Wang et al. (1994) found that the flow rates in small vertical and continuous macropores caused by earthworms were very high compared with the flow rates in the matrix. In this type of macropores, flow rates higher than the rainfall intensity were observed.

Weiler (2001) studied the main processes controlling macropore flow, emphasizing in the initiation of the flow and the interaction between the flow through macropores and the matrix. This author conducted a number of studies based on sprinkler experiments to analyze flow in macropores caused by earthworms in grassland soils. Outcomes of these studies showed that the influence of macropores on infiltration depend mainly on the initiation of the flow and its interaction with the matrix flow. The permeability of the soil surface was found the major issue influencing the initiation while the soil water content was considered the main factor on the interaction between the two hydrological domains.

Dye tracers have been used for identifying flow paths and quantifying preferential flow in grass soils (Weiler & Naef, 2003). In a different way, conservative tracers have been used to identify differences in flow magnitudes and flow velocities trough macropores and the matrix. Some experiments carried

out in a waste water treatment pond used an instantaneous application of Br^-. There, the analysis of the breakthrough curve at the outlet of the pond, which showed consecutive peaks of the tracer allowed the characterization of different flow paths (Maloszewski et al, 2006). In other experiments, the analysis of the different flow domains was done from breakthrough curves that are representative of every domain (Weiler & Naef, unpublished). A similar approach with isotopes was applied by Stumpp et al. (2007).

2.3. HYDROLOGICAL MODELLING IN SUPER-SAUZE LANDSLIDE

The spatially-distributed and physically-based model STARWARS (STorage and Redistribution of Water on Agricultural and Re-vegetated slopes) was adapted to incorporate a conceptual hydrological model defined for the Super Sauze landslide. Three hydro-geomorphological units were used for this model. These units were defined by differences in displacements and in their hydrological behaviour. Unit HG1 is the most dynamic part, HG2 is a zone of accumulation of material in the lower part of the landslide and HG3 correspond to the area with least displacement, namely the stable area. The units are shown in Figure 2.1 and their main characteristics are mentioned in table 2.1.

Table 2.1 Hydro-geomorphological units used in the STARWARS model

Hydrological characteristic	Unit name		
	HG1	HG2	HG3
Piezometric response time	Very rapid (<1 h)	Rapid (2– 3 h)	Slow (>5 h)
Fluctuation	Significant (up to +0.4 to 0.5 m)	Moderate (+0.05 to +0.3m)	Low (centimetric)
Drainage time	Rapid (3-5 h)	Relatively rapid (12–24 h)	Slow (>24 h)

The results of the STARWARS model were satisfactory for the drainage and the range of groundwater levels but produced delays in the time of groundwater recharge. The need of more detailed spatial representation of hydraulic conductivity, porosity and the density of fissures was identified in order to improve the understanding of the recharge from precipitation. These changes could lead to a redefinition of the hydrological response units.

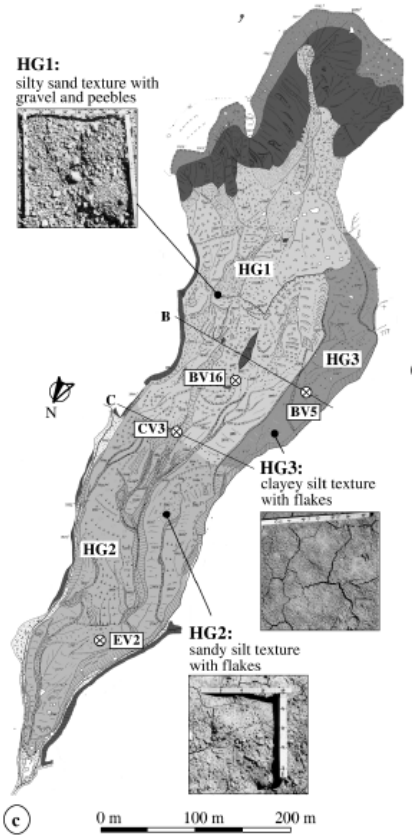

Figure 2.1 Map of units used for STARWARS model (From Malet et al., 2005)

3. METHODOLOGY

In this chapter, the applied methods and the data used in this study are described. The chapter is divided into four sections; the first deal with geomorphological and spatial analysis; the next two relate to the hydraulic characterization of materials and its spatial generalization; and the last one refers to the analysis of sprinkler test.

Part of the data used for this study was obtained during two weeks of field work at the Super Sauze landslide site on October of 2008. These data include a set of geomorphological descriptors and the results of geotechnical and hydrological tests used to characterize the soil materials. Additionally, data from three sprinkler tests performed by researchers from the Delft University of Technology and a detailed ortho-mosaic of the landslide made as part of an investigation from Stuttgart University were used.

3.1. GEOMORPHOLOGICAL CHARACTERIZATION AND MAPPING

Geomorphological characterization during the field work was done to build an updated map that contains the main features of the landslide, including the location and description of tension-induced cracks. Areas with different geomorphological characteristics within the landslide were geo-referenced and described. The description for each area includes its approximate size, the aspect and angle of the slope, the rock size and extent of rock cover, and the presence or absence of fissures. Additionally, measures of maximum soil resistance to penetration, bulk density and soil moisture were done in some areas. In areas with fissures, their size, density, and main orientation was also measured. The described fissures were the ones easily identifiable in the soil surface, having widths on the order of tenths of centimeters and lengths on the order of meters; smaller fissures were not included.

Identification codes were given to the areas, consisting of consecutive numbers assigned from higher to lower altitudes, plus letters indicating the presence or absence of fissures. The methods used to characterize the areas are mentioned in table 3.1.

Table 3.1 Geomorphological descriptors

Descriptor		Unit	Method of measurement or evaluation
Location	coordinates	[m]	Measured on one point inside every area with a GPS receiver and later projected to Lambert III coordinate system
Slope	type	[-]	Visual
	angle	[-]	Measured with a compass in a representative place of the area
Lithology	rocks cover	%	Estimated on detailed pictures taken during the field work
	rocks size	[L]	Mid diameter estimated on detailed pictures taken during the field work
Fissures	The size of the fissures was measured in randomly selected points within any area.		
	Open depth	[L]	The empty depth of the fissures was measured with a metric tape
	Filled depth	[L]	Filled depth, measured with a stick of 1.5 m inserted in the soil
	Total depth	[L]	Sum of open and filled depths
	Width	[L]	Width of the fissures measured perpendicular to the main direction of the fissures
	Density	[#/L]	Number of fissures along 5m length, counted perpendicular to the main direction of the fissures
Max strength		$[F/L^2]$	Hand penetrometer at 25, 50, 75 and 100 cm depth
Bulk density		$[M/L^3]$	Core method

The maximum resistance to penetration was measured with a hand penetrometer which measures the maximum resistance force of the soil on a cone of known area. The resistance to penetration (kN/cm^2) of the soil is determined by dividing the reading value by the surface of the cone being used.

$$\max R = \frac{F}{A} \qquad [3.1]$$

Where,

max R	Maximum resistance (kN/cm^2)
F	Reading measure (kN)
A	Area of the cone (cm^2)

The fraction of every geomorphological unit that consists of open spaces caused by fissures was calculated as the average width of the fissures times the density, as illustrated in figure 3.1.

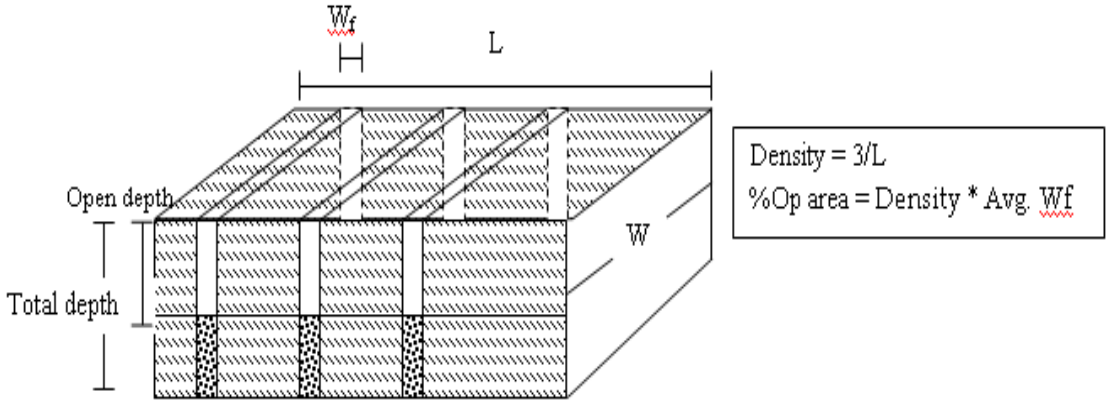

Figure 3.1 Representation of fissures size and density

The delineation of the geomorphological areas described above, was done by using a high resolution ortho-mosaic as background. This mosaic was built by researches from Stuttgart University and is based on photos taken from an unmanned aerial vehicle (UAV) simultaneously with the field work. It covers the whole area of the landslide with a maximum resolution of 3 cm (Niethammer et al., 2009).

The values of the geomorphological descriptors from the field work were included in attributes tables, making possible to create maps of individual or combined characteristics. Additionally, the observable fissures were delineated on a map with the purpose of identify their extension, connectivity and pattern distribution.

3.2. SATURATED HYDRAULIC CONDUCTIVITY AND SOIL MOISTURE

The saturated hydraulic conductivity (Ks) was measured in the soil matrix and in the soil material which fill partially the fissures. This material will be referred to as fissures in the following sections. The inversed auger hole method was used in the unsaturated matrix material, whereas a modified inversed auger hole method was used for measurements in the fissures.

In addition, soil moisture was measured at the surface and at variable depths up to one meter, in 14 selected places. Eight points were located in the stable part and two more points were located at each sprinkler experiment plot.

3.2.1. Inversed auger hole method

The saturated hydraulic conductivity was measured using the inversed auger hole principle (Kessler and Oosterbaan, 1974), that is a saturated permeability test in the unsaturated zone in a shallow open borehole (Figure 3.2).

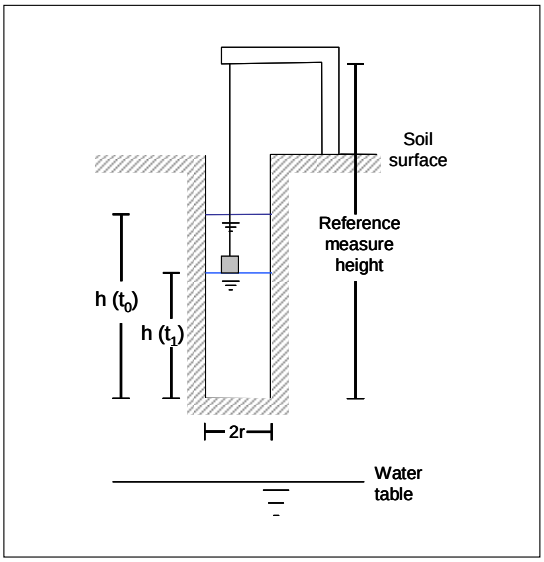

Figure 3.2 Inversed auger hole test

Having *r* as the radius of the borehole and *h* as the height of water above its bottom, the wetted surface A is calculated as $A = 2\pi h + \pi r^2$. It is assumed that during the test, the hydraulic gradient equals one. Ks is calculated as follows:

According to Darcy's equation

$$Q = K_s A(t) i = 2K_s \pi r (h + \frac{1}{2} r) \times 1 \qquad [3.2]$$

which combined with the continuity equation

$$Q = -\pi r^2 \frac{dh}{dt} \qquad [3.3]$$

yields

$$K_s dt = \frac{-\frac{1}{2} r * dh}{h + \frac{1}{2} r} \qquad [3.4]$$

Integrating equation 3.3 for h = h_1 at time t = t_1 and h=h_n at time t=t_n gives

$$K_s = \frac{2.3}{2} \times r \times \frac{\log\left(h_1 + \frac{1}{2} r\right) - \log\left(h_n + \frac{1}{2} r\right)}{t_n - t_1} = 1.15 \times r \times \tan\alpha \qquad [3.5]$$

Where

K_s Saturated hydraulic conductivity [LT^{-1}]
r Radius of the borehole [L]
t_1 Starting time [T]
t_n Final time [T]
h_1 Height of water above the bottom of the borehole in time 1 [L]
h_n Height of water above the bottom of the borehole in time n [L]

tangent α is obtained from a linear regression of (log(h) + ½ r) vs. time from the last part of the test where the function approximates a straight line.

3.2.2. Modified auger hole method

Due to the limited width of the fissures and the expected higher permeability, a modified form of the auger hole method was used in the fissures. For this, PVC access tubes with filters of known lengths were used; in this way it was possible to measure the local Ks at chosen depths. Infiltration took place only through the lateral area of the filter since the bottom was closed.

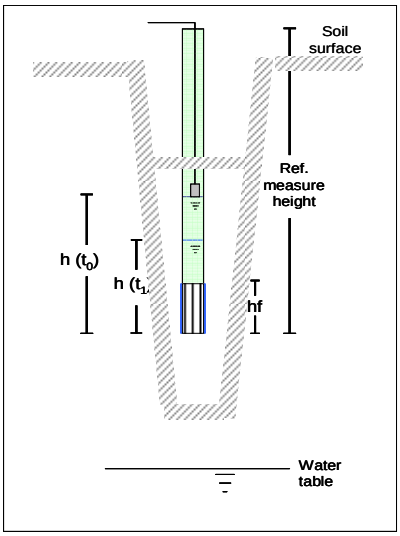

Figure 3.3 Modified inversed auger hole test

To install the PVC tubes, holes were dug with a manual soil drill. Then the tubes were inserted into the soil using a rubber hammer. The diameter of the dig hole was slightly smaller than the diameter of the tube, thus allowing good contact between the filter and the material of the fissures, so there was no need to use sand filters.

The equation of conservation of energy and the equation of conservation of mass are equaled to calculate Ks as follows:

$$Q = K_s A(t) = K_s 2r\pi h(t) = \frac{dh}{dt}\pi r^2 \qquad [3.6]$$

what yields,

$$K_s = \frac{r}{2h} \times \frac{dh}{dt} \qquad [3.7]$$

Where

h The length of the filter [L] when the level of water is above the filter and the average of h_t and h_{t-1} when the water level is below that level.

Ks from every test is calculated as the average of Ks at different time steps, from the last part of the test where the relation of h vs. t approximates a line.

3.2.3. Soil moisture content

Soil moisture was measured at the surface with a manual Delta-T device type ML2 provided with pins of 5 cm. Measurements were done below the surface with an integrated theta probe rod type PR1, at depths of 10, 20 30, 40, 60 and 100 cm using previously installed access tubes.

3.3. SPATIAL GENERALIZATION OF Ks

The first approach to scale the values of Ks from specific areas to the landslide extension is to evaluate the possibility of relationships between Ks and the described geomorphological characteristics. It is assumed that these characteristics are representative for different types of soil structure and soil particle sizes, hence for the saturated hydraulic conductivity.

Initially, classes of the geomorphological descriptors were defined in order to look at qualitative relations between these geomorphological parameters and Ks. In a further step, qualitative analysis was done using the geometric mean of Ks and numerical geomorphological descriptors.

The second approach was the use of probability density functions. The measured Ks in the fissures and in the matrix were analyzed to define the type of probability distribution they follow. The analysis was done with the software application BEST FIT, which optimizes 18 probability functions, runs the Chi-square, Kolmogorov-Smirnov and Anderson-Darling tests of fit, and ranks the calculated distributions, according to the values of the tests.

The tests in which immediate drainage occurred were used to calculate the probability of preferential flow as:

$$P(PF) = \frac{\#PF}{\#T} \qquad [3.8]$$

Where

P(PF) Probability of preferential flow
#PF Number of tests with immediate drainage
#T Total number of tests

The total probability, which combines the probability of preferential flow and the probability of flow in porous media, is calculated with the total probability theorem as follows:

$$P(K) = P(K \perp MF)P(MF) + P(K \perp PF)P(PF) \qquad [3.9]$$

Where

P(K)	Probability of Ks
P(K | MF)	Probability of Ks given matrix flow
P(MF)	Probability of matrix flow
P(K | PF)	Probability of Ks given preferential flow

3.4. SPRINKLER TESTS

Three sprinkler tests were carried out on July 2008 in three different locations along the Super-Sauze mudslide. One in the upper part, just below the main scarp of the landslide; another in the area with less displacements, namely the stable area and the last one, in a deposit area, in the most dynamic part of the landslide. These locations feature different dynamic behavior and were expected to show markedly different hydraulic responses.

The tests were performed in plots of 1 m^2 named A, B and C in order of decreasing altitude. Artificial rain was sprinkled on the plots, in 15 minute periods, alternating between rainfall and no rainfall, over 7 to 8 hours on 2 consecutive days. The applied rainfall was measured with 5 small rain gauges located within the plots (appendix 1). Later, the areal distribution of rain was calculated with the Thiessen polygon method.

In order to protect the experiments from wind disturbances and to minimize evaporation, the rained areas were covered with tents. At each plot, 4 piezometers were installed: one in the middle of the plot, and the other three outside of it. Two of these piezometers were located in the direction of the expected subsurface flow and the other, upslope of the plot. Additionally, 2 theta probes of 1 m length were installed laterally to the plots in areas A and C.

Water levels were monitored continuously with three minutes interval using pressure transducers, and manual measurements were performed every 30 minutes.

The conservative tracers Br^- and Cl^- were applied with the artificial rain to trace infiltration processes. The water sampling from the piezometers was done manually every hour and analyzed in the laboratory afterwards.

3.4.1. Water balance

The general formula of the water balance is the following, however not all components occur in every plot:

$$P + GW\text{-}in = GW\text{-}out + OF + E + SSF + \Delta S / \Delta t \qquad [3.10]$$

Where

P	Applied rain [L^3/T]
GW-in	Groundwater inflow [L^3/T]
GW-out	Groundwater outflow [L^3/T]
OF	Overland flow [L^3/T]
E	Evaporation [L^3/T]
SSF	Subsurface flow [L^3/T]
$\Delta S / \Delta t$	Change in storage [L^3/T]

The volume for calculating the water balance for the sprinkler tests is determined by the rained-on plot area of 1 m^2, and the maximum depth of the piezometer in the center of each plot. The water balance was first calculated for time steps of three minutes and afterwards summed up on a daily basis.

GW-in is considered to be equal to GW-out. E is considered negligible because the area of the experiments was covered by a tent which also avoided wind disturbances. SSF comprises exfiltration, vertical and lateral flows.

The change in storage is calculated at every time step after Nonner (2002):

$$\frac{\Delta S}{\Delta t} = AS_y \frac{dh}{dt} \qquad [3.11]$$

where

h(t)	Water level above a reference level at time t [L]
A	Area [L^2]
Sy	Specific yield [-]

The value of the specific yield is iterated so that the cumulative change in storage is near to zero at the end of the drawdown, and the values of storage calculated by two different methods give similar results. The total change in storage is calculated from the beginning of the experiment until the end of the drawdown. The storage at the end of the last rain is calculated in two ways, one is obtained from the water balance and the other is computed as the maximum storable volume of water, defined by the porosity minus the initial water content,

according with equation 3.12. The difference on the results of these two methods is calculated as a percentage of error.

$$S(t) = (n - \theta) \times A \times h(t) \qquad [3.12]$$

Where

S(t) Storage at time t [L^2]
n Porosity [-]
θ Initial soil moisture content [-]

The values of specific yield are maintained in the range of the porosity minus the initial soil moisture content. The values of porosity were taken from previous measures of the Mountain Risks project while the soil moisture content is taken from the measurements of the theta probe rods during the experiments and during the field work.

Data processing was done, including the filling of short segments of missing data on the series of water levels, by linear regression, and the correction of the drawdown caused by the water sampling for chemical analysis.

3.4.2. Tracer's analysis

The concentrations of the conservative tracers Br^- and Cl^- were used in the experiments to identify the infiltration paths and to calculate the proportions of different sources of water in specific locations, with the following mass balance equations:

$$V_T = V_1 + V_2 + ... + V_n \qquad [3.13]$$

$$C_T V_T = C_T V_T + C_T V_T + ... + C_n V_n \qquad [3.14]$$

Where

VT Total volume [L^3]
V1...n Volume of different sources of water [L^3]
CT Concentration in the final volume [M/L^3]
C1...n Concentration of any of the sources [M/L^3]

3.4.3. Quantification of preferential flow

The analysis of the drawdown curves after the end of the rain is done similarly to hydrograph recessions. This allows the identification of different hydraulic domains. The hydrograph recession analysis has been used in other studies of preferential flow (Mikovari & Leibundgut, 1995; Scanlon et al., 2000).

In this study the method is applied to identify differences in types of storages, from the occurrence of inflexion points in the drawdown curves. The method is used under the assumption that the change in water levels is a direct function of change in drained volumes and therefore, of a change in storage. The reservoirs are assumed linear, that is they have an outflow proportional to the storage.

The empirical method is explained by de Laat (2006) and Linsley et al., (1982) where the parameter to be fixed in equation 3.15 is the recession constant K.

$$h_t = h_o e^{-\frac{t-to}{K}} \qquad [3.15]$$

K indicates the time for depletion of every storage and is calculated for each segment of the drawdown curve defined by inflexion points. The steeper part of the curve represents fast drainage, assumed to be preferential flow, whereas the less steep part of the curve represents slower drainage, comparable to matrix flow. After the inflexion point it is presumed that the preferential flow have stopped. K is calculated for every storage by the minimum square error method.

Afterwards, the curve correspondent to the slow drainage is projected until the beginning of the drawdown. This curve is used to calculate Darcy's flow at every time step between the piezometer at the center of every the plot and the piezometers outside the plot. Later, the accumulated matrix flow is calculated as the sum of the flows of every time step.

Finally, the ratio of the matrix flow to the storage at the end of the last rain, taken from the water balance, is calculated. An estimation of the total drainage by the matrix is obtained by multiplying the calculated drainage from the first 15 minutes by the duration of the experiment. This period is selected because it is representative of the fluctuations of head that are repeated at the occurrence of each rain block.

4. GEOMORPHOLOGICAL AND HYDROLOGICAL CHARACTERIZATION OF SUPER SAUZE LANDSLIDE

4.1. DESCRIPTION OF THE STUDY AREA

The Super-Sauze is a deep-seated earthflow located in the French Alps about 100 km north of Nice (Figure 4.1). It has a horizontal extension up to 820 m and occurs between elevations of 1740 and 2015 meters above sea level (masl). The total volume is estimated as 750.000 m^3 and the displacements occur in the range of 0.01 to 0.4 meters per day (Malet et al., 2005).

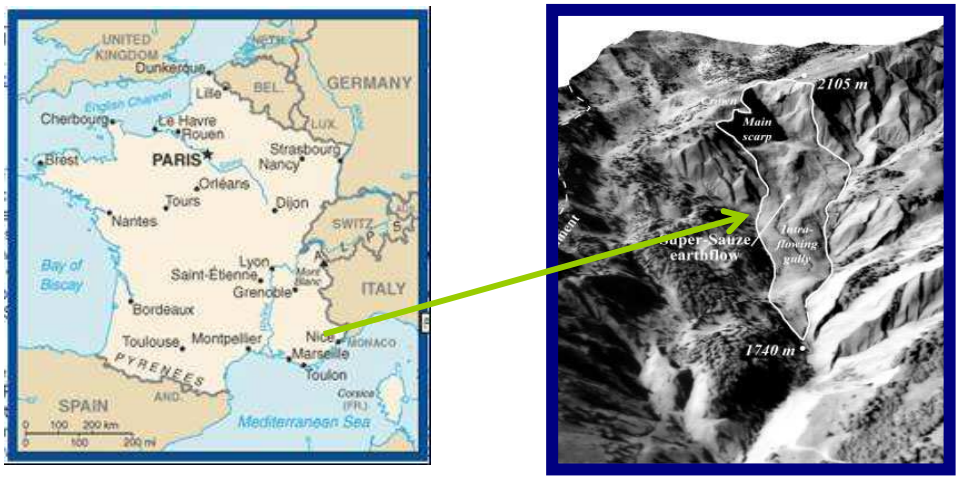

Figure 4.1 Location of Super Sauze landslide

Geotechnical investigations indicate that the earthflow has a maximum depth of 20 m and "fossilizes an intact palaeotopography formed by a succession of *in situ* Callovo-Oxfordian black marl crests and gullies. The palaeotopography strongly influences the behaviour of the flow by delimiting compartments with different characteristics and creating preferential water and sediment pathways." (Malet et al., 2002). The earthflow comprises reworked blocks and panels of marls at different stages of weathering, clasts of all sizes, a silty-clayed matrix, and some morainic blocks. The soil materials are affected by cracking due to mechanical tension or desiccation.

Vegetation is limited to patches in very few locations. The area is characterized by very variable rainfall (400 to 1300 mm/year), intense summer and autumn storms, which can reach intensities of 50 mm/h in 15 min, snow cover and freezing for 130 days per year on average (Malet et al., 2002).

4.2. GEOMORPHOLOGICAL CHARACTERIZATION

The main features identified in the landslide, from the field work recognition, include a stable area; an area with slow movement and accumulation of debris near the toe of the landslide and, the most dynamic area formed by two big mudflows separated by a central crest. The surface of this crest is covered by material comprised of blocks of marls and blocks from the moraine which range from some centimeters to more than one meter. Additionally, two perennial torrents surrounding the landslide were identified.

Beyond these main features, more detailed units were identified. They include a number of flows, slides and gullies occurring along the landslide, as well as their constitutive areas. These areas were delineated using Arc Map, taking the detailed ortho-mosaic as background. The upper part of the landslide was group as one unit, although various types of movements occur in combination and in small extensions. This unit is called the upper part for the purposes of this report (Figure 4.2).

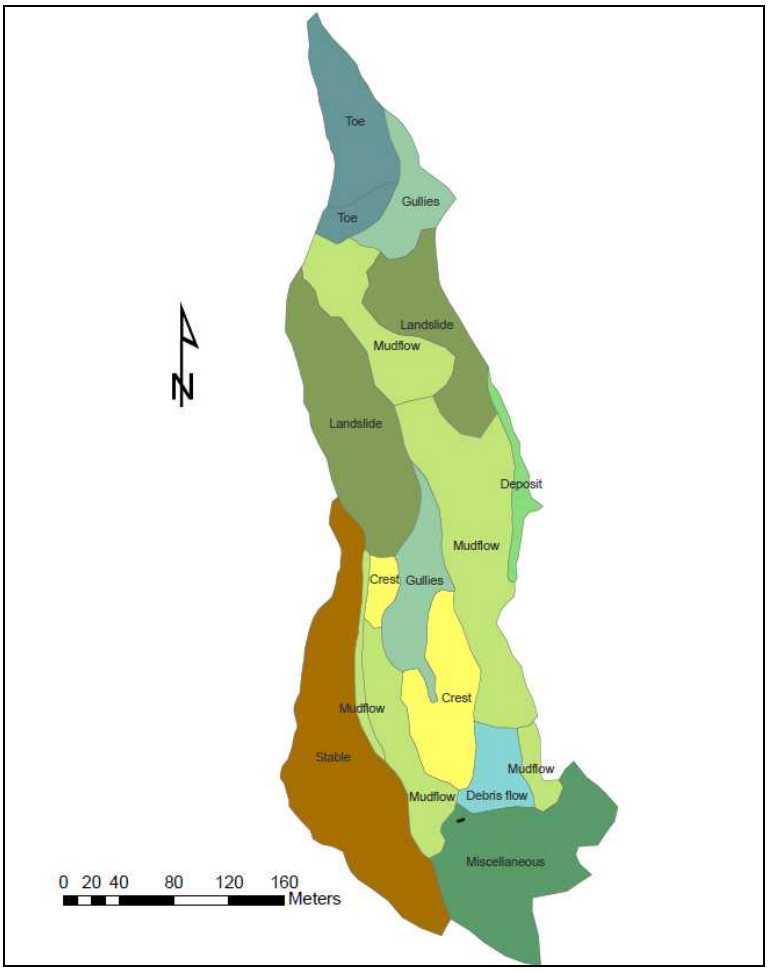

Figure 4.2 Map of geomorphological units

The tests of maximum resistance to penetration showed differences between the matrix and fissure materials. While in the fissures, it was in general possible to measure to depths of 1 m, in the matrix it was only possible to 0.50 m in most areas. This is because the resistance was higher than the maximum applied force or due to the presence of rocks. The average measured resistances are shown in table 4.1.

Table 4.1 Maximum resistance to penetration

Depth (m)	Max resistance (KN/cm^2)	
	Fissures	Matrix
0.25	0.11	0.38
0.50	0.13	0.38
0.75	0.14	
1.00	0.17	

In appendix 2 are the values descriptors of the units as well as their distribution according with a classification specified for these descriptors.

The geomorphological characterization revealed that areas with gentle slopes of about 20^o have planar shapes and correspond to the deposits of mudflows. The fissures located in this type of areas are narrow and deep. Conversely, the steepest slopes up to 45^o have a convex shape and occur on crests and on the heads of landslides and flows. The biggest fissures are located in this kind of areas.

Furthermore, it was found that in eight units, the average depth of the fissures is more than 1 m and in five of them the open depth is more than 0.5 m. In addition, the percentage of open spaces is more than 50% in three units; in these units the existent fissures have depths more than 1 m and widths more than 0.2 m.

The spatial analysis allowed the visualization of the main geomorphological features which comprise the upper part of combined type of movements, the stable area in the south western part, two main flows separated by the central crest (Figure 4.3). These flows occur continuously along the landslide by successive areas of sources, tracks and deposits. Additionally, some intermittent gullies were identified. The ones located in the stable part have clearly differentiable channels whereas the others are very superficial, and partly filled with soil materials.

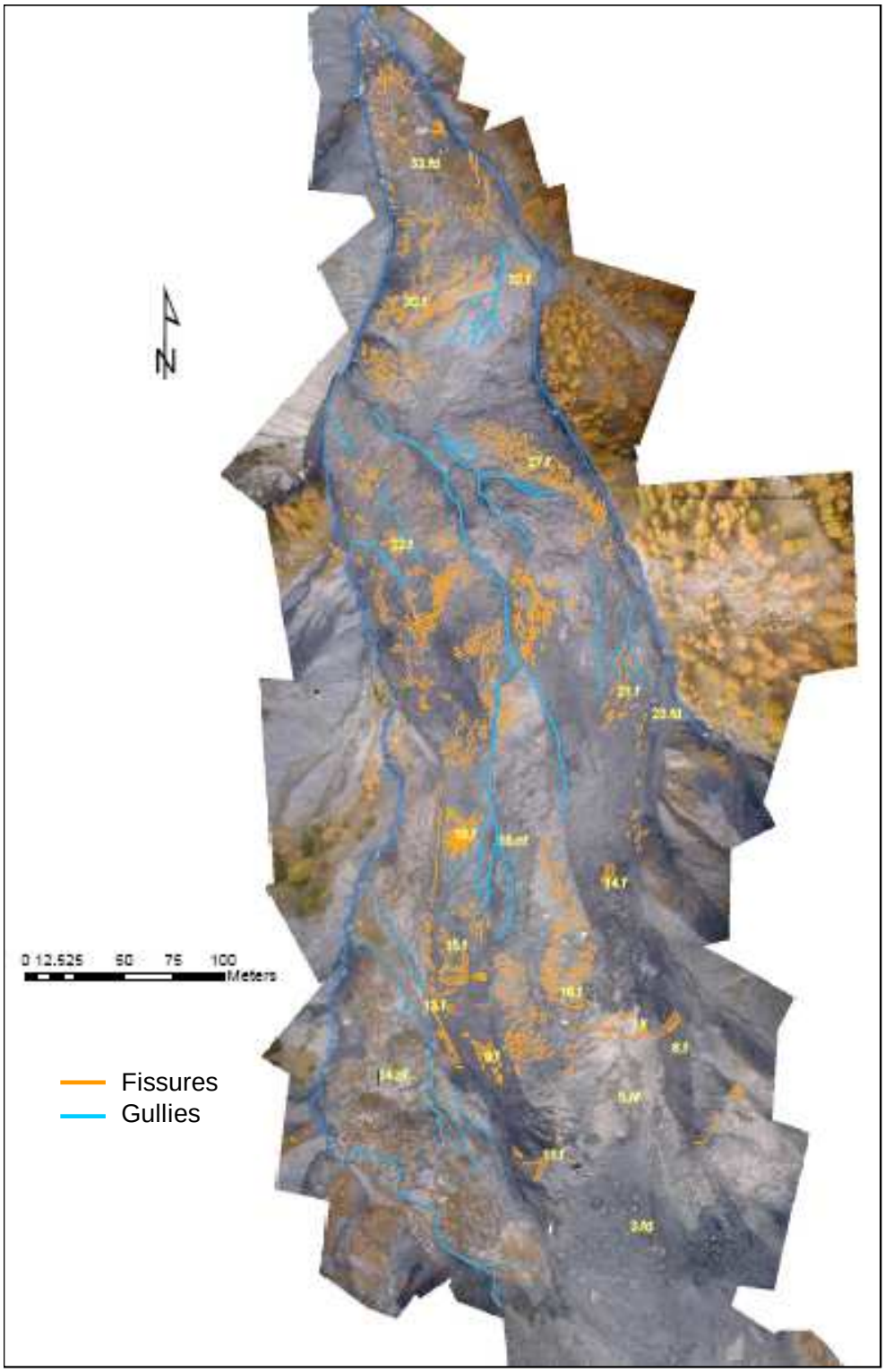

Figure 4.3 Map of distribution of fissures

The largest fissures occur on the crests and on the crowns of some slides and flows located in upper half of the landslide area. Most of them have radial

patterns and lay perpendicular to the local and general slope, as in areas 6.f and 11.f. These areas were also found to be the longest, up to 35 m. High groundwater levels were observed in this kind of fissures during the first days of fieldwork which was a very dry period. On the following days an accumulation of rain was observed, until some hours after the stop of the rain and accumulation of snow on the open spaces of the fissures until the soil surface. The fissures in the deposit area 15.f have the same type of position.

Conversely, other fissures lay parallel to the local slope. Some long fissures up to 10 m like in the central crest and shorter ones mainly in deposit areas like 21.f and 27.f which run parallel to the intermittent gullies. In the areas at the sides of the two main flows, there are short fissures which lay diagonal to the slope.

The area where fissures are present is 35000 m^2, near 50% of the area of the landslide. In more than half of this extension fissures are medium deep and narrow fissures, i.e. have depths lower than 0.5 m and width lower than 0.2 m narrow fissures. In one fourth fissures are deeper than one meter and wider than 0.2 m; in the rest of the area deep and narrow fissures and filled fissures are present.

4.3. SATURATED HYDRAULIC CONDUCTIVITY ANALYSIS

Infiltration tests were carried out in 19 of the areas described in the previous section, in both fissures and matrices. A total of 217 tests were done; 125 in the fissures and 92 in the matrix.

Tests were performed in the matrix at depths from 17 to 62 cm, while in the fissures, these ranged from 15 to 75 cm. A summary of the number of analyzed tests is presented in Table 4.2.

Table 4.2 Summary of infiltration tests

Location	Matrix			Fissures		
	Number of tests	Calculated Ks	Immediate drainage	Number of tests	Calculated Ks	Immediate drainage
3.fd	4	3	1	4	0	4
6.f	5	3	0	9	8	0
7.f	0	0	0	8	5	3
8.f	5	5	0	5	2	3
9.f	4	3	0	10	10	0
13.f	0	0	0	5	5	0
15.f	7	6	0	12	5	6
16.f	5	5	0	8	4	3

Location	Matrix			Fissures		
	Number of tests	Calculated Ks	Immediate drainage	Number of tests	Calculated Ks	Immediate drainage
17.f	7	6	0	15	11	4
18.nf	7	3	0	0	0	0
19.f	5	2	0	4	0	4
21.f	5	3	0	16	16	0
22.f	5	3	0	7	1	5
23.fd	7	5	0	2	2	0
24.nf	7	5	1	0	0	0
27.f	6	6	0	14	5	9
30.f	5	3	2	6	0	2
33.nf	5	1	4	0	0	0
34.nf	3	3	0	0	0	0
Total	92	65	8	125	74	43

Some tests could not be analyzed because the limited measured points of dh/dt or due to the absence of a linear relation of (log(h(t)+r/2) vs. time. The qualitative value "Immediate drainage" was assigned to tests where water infiltrated completely in a very short time, i.e. less than 60 seconds. In these cases the very fast drainage is understood as occurring through macropores.

It is worth noting that 35% of the tests performed in the fissures materials have immediate drainage whereas this phenomenon only occurred in 8% of the tests in the matrix.

4.3.1. Ks in the soil matrix

There appears to be great variability among the whole group of calculated Ks in the matrix, ranging from 7.51×10^{-3} m/day to 3.18×10^{1} m/day, with a mean of 3.79 m/day and a standard deviation of 7.76 m/day. There is no linear correlation of Ks with depth in the measured range, and no indication of any other kind of relationship (Figure 4.4).

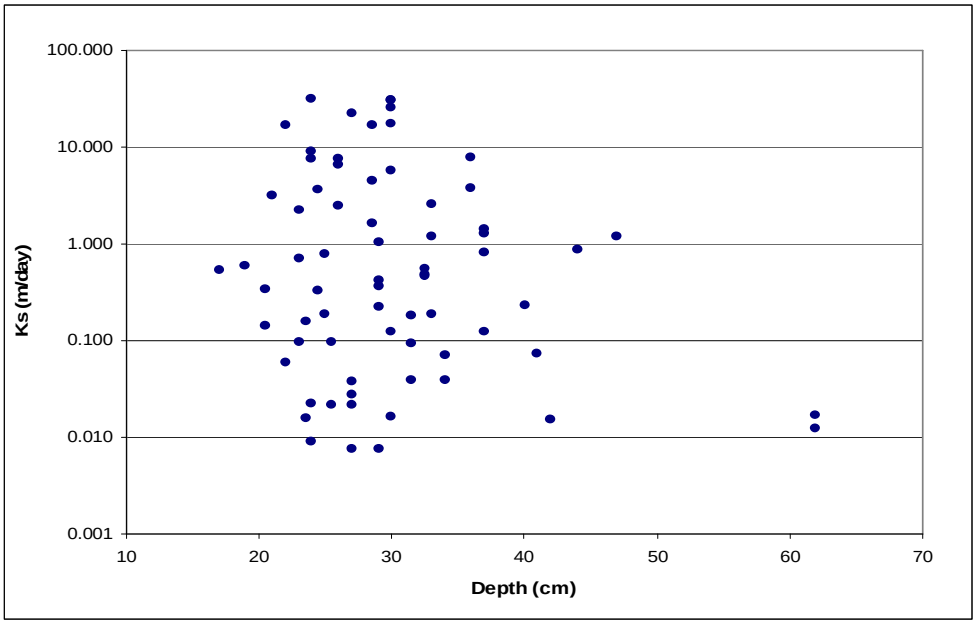

Figure 4.4 Saturated hydraulic conductivity in the matrix

The geometric mean, the coefficient of variation (CV) and the correlation coefficients (R) of Ks with the maximum depth of the tests are presented in table 4.3.

Table 4.3 Statistical descriptors of Ks in the matrix

ID	Geo_mean Ks [m/day]	CV [-]	R Ks-depth [-]
3.fd	12.93	0.84	NC
6.f	0.03	1.12	-1.00
8.f	0.07	1.14	-0.73
9.f	0.03	1.09	-0.09
15.f	3.97	1.24	-0.62
16.f	0.59	1.28	-0.73
17.f	0.31	0.98	0.68
18.nf	0.29	1.64	0.67
19.f	1.02	0.22	NC
21.f	0.02	0.72	0.92
22.f	0.52	0.64	0.60
23.fd	0.13	1.08	-0.79
24.nf	2.76	1.02	-0.55
27.f	0.46	1.71	0.07
30.f	7.08	0.86	0.95
33.nf	NC	NC	NC
34.nf	0.67	1.37	-1.00

The correlation coefficient was not calculated in some areas, indicated as NC, because in these cases, less than 3 values of Ks were calculated, or all the tests were done at the same depth.

A negative linear correlation of Ks with depth greater than 0.6 was found in 5 of the 14 areas. On the other hand, in most of the areas the coefficients of variation are higher than one in most of the areas.

4.3.2. Ks in the fissures

The values of Ks found in the fissures were also found to have great variability, ranging from $1.26x10^{-2}$ m/day to $2.43x10^{1}$ m/day. The average Ks is 2.89 m/day and the standard deviation is 4.88 m/day. The correlation coefficients of Ks and the depth of the tests in the fissures is slightly higher than in the matrix, but still lower than 0.3 (Figure 4.5).

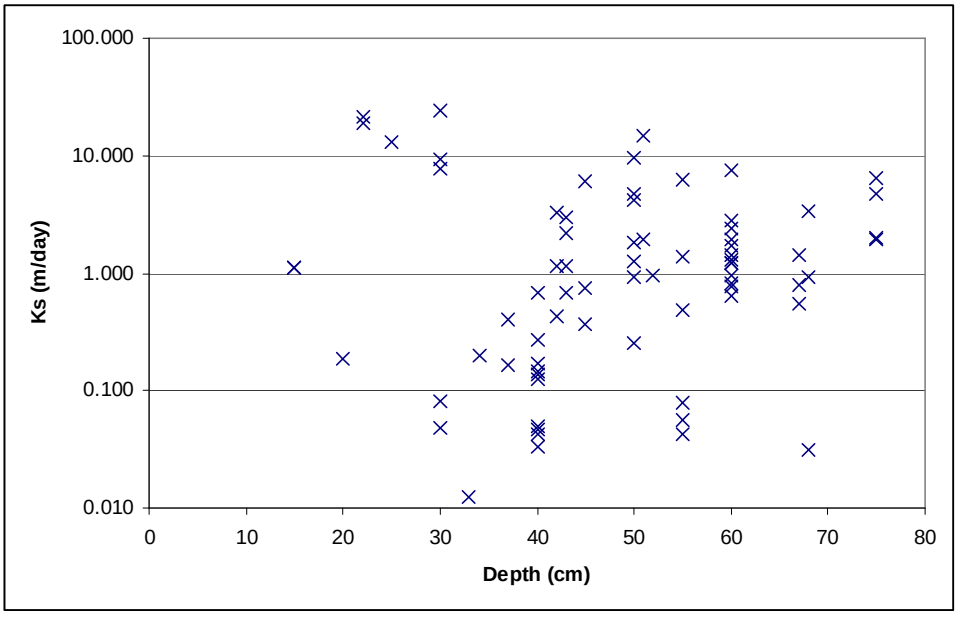

Figure 4.5 Saturated hydraulic conductivity in the fissures

Descriptors of central tendency and variation are presented in the following table (Table 4.4).

Table 4.4 Statistical descriptors of Ks in the fissures

ID	Geo_mean [m/day]	CV [-]	R Ks-depth [-]
8.f	8.96	0.52	NC
6.f	0.27	0.98	-0.90
7.f	0.42	0.76	0.61
16.f	4.53	0.93	-0.35
15.f	2.55	0.99	-0.64
9.f	1.82	0.78	0.47
13.f	0.53	1.57	-0.87
17.f	1.00	0.71	0.24
21.f	0.37	1.54	NC
27.f	3.28	1.21	-0.97
23.fd	0.20	0.04	NC

There is a negative correlation higher than 0.6 in 3 of 11 areas. Therefore, Ks does not show dependency on depth in most of the analyzed areas in the surveyed depth.

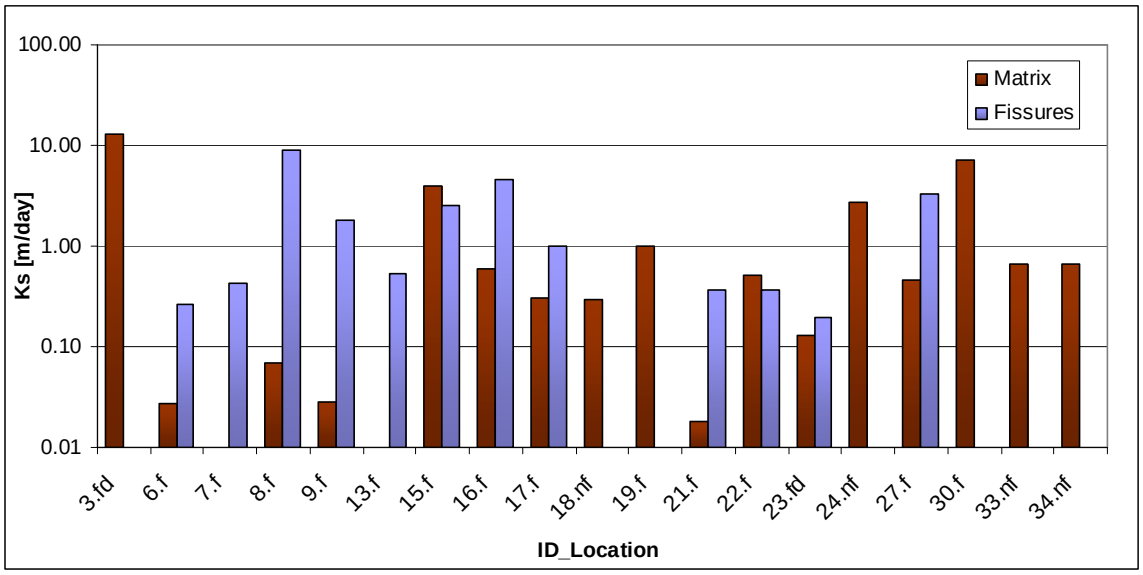

Figure 4.6 Ks in matrix and fissures materials

It can be noticed that Ks in the matrix is lower in all the areas than Ks in the fissures materials, with exception of areas 15 and 22, however in both of these areas preferential flow in the fissures materials occurred in more than 50% of the tests.

4.3.3. Previous measurements of Ks

Values of Ks calculated on this research were compared with previous measurements. The previous data set consists of 153 measurements taken in 25 locations from 1999 to 2002 (Figure 4.7).

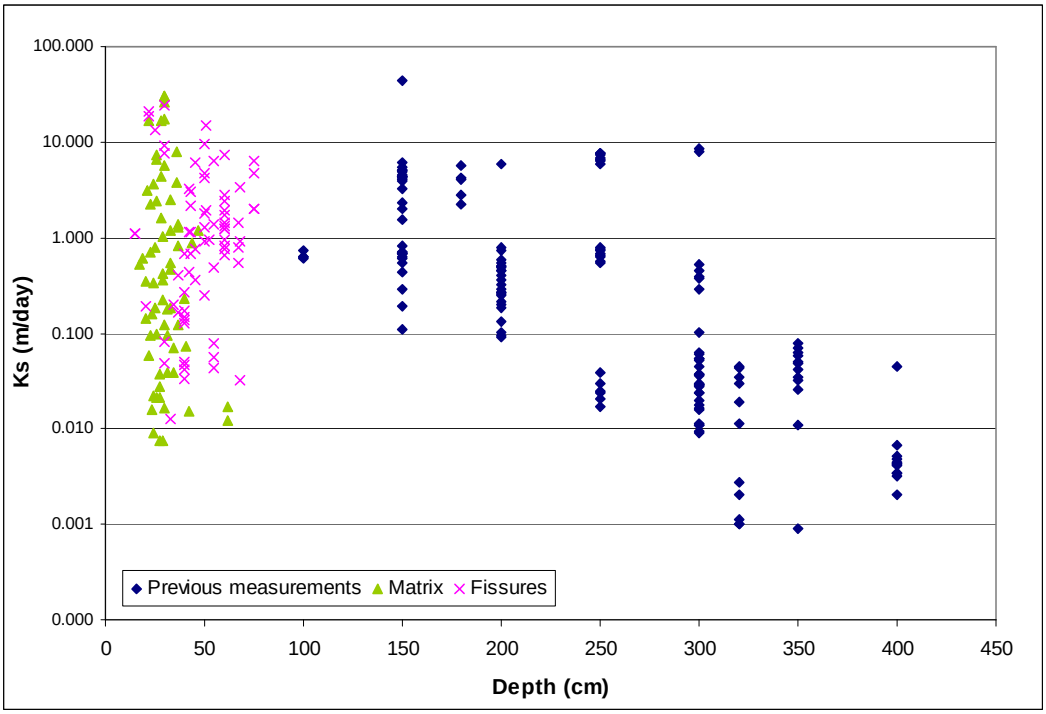

Figure 4.7 Saturated hydraulic conductivity from different sets of data

From the plot, it can be observed than in all sets, most of the Ks values are between 10^{-3} and 10^{1} m/day. These values are characteristic of sandy clay to fine sand soils (Nonner, 2002), thus they are high for the silty-sand texture characteristic of Super-Sauze.

The next histogram shows that most of the Ks in the fissures have values between 10^{0} and 10^{1} m/day whereas in the matrix most are located between 10^{-1} and 10^{0} m/day.

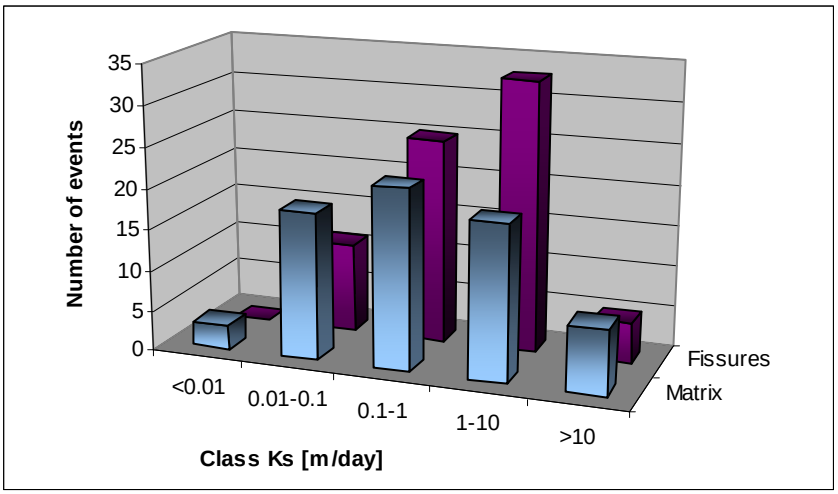

Figure 4.8 Histogram of Ks in the matrix and fissures

4.4. SPATIAL DISTRIBUTION OF Ks

A classification of the values of Ks was done with the purpose of define relations of this parameter with the geomorphological descriptors. Three classes were defined: low, high and variable (Table 4.5). The limit of the low and high classes is rather arbitrary; it was defined as 10 m/day, based on the classification of Bear (1972) who consider this as the limit between permeable and semi-permeable unconsolidated materials.

The areas were assigned to a class when more than 80% of the data were in the range of values or, in the case of the high variability class, when the coefficient of variation was higher than one and Ks varies by more than two orders of magnitude.

Table 4.5 Description of hydrological classes

Class	Ks fissures (m/day)	Ks matrix (m/day)
Low	0.01 < Ks < 10	0.001 < Ks < 10
High	Ks > 10	Ks > 10
Variable	High variability	High variability

Table 4.6 shows the distribution of the areas in the defined classes, showing that most matrix areas fit in the low permeability class, and fissured areas in the variable class.

Table 4.6 Distribution of the areas in hydrological classes

	Ks Fissures			
Ks Matrix	Low	High	Variable	No test in fissures
Low	9.f 23.fd	8.f 19.f	6.f 16.f 21.f 22.f	
High		3.fd 30.f		
Variable			15.f 17.f 27.f	18.nf 24.nf 34.nf
No tests in matrix			7.f 13.f	

In both areas with filled fissures, those which are filled with material up to a few centimeters from the surface, Ks of fissures and matrix materials remain in the same class.

In the following table the classes of Ks are distributed according with the size of the fissures, but no correlation was found. The classes of the fissures size are described on appendix II. The only observation of note is that a high number of areas are located in the category denoting variable Ks and medium deep - narrow fissures.

Table 4.7 Relation of Ks and fissures size

	Fissures size			
Ksat	Medium deep - narrow	Deep - narrow	Deep - wide	Filled
Low		9.f		23.fd
High	8.f 30.f		19.f	3.fd
Variable	7.f 13.f 15.f 17.f 22.f 27.f	21.f	6.f 16.f	

No correlation was found between the geometric mean of Ks and other numerical descriptors of the areas. As examples, plots of the geometric mean of Ks against the average width of the fissures and the percentage of open fissures in the areas are included in figure 4.9.

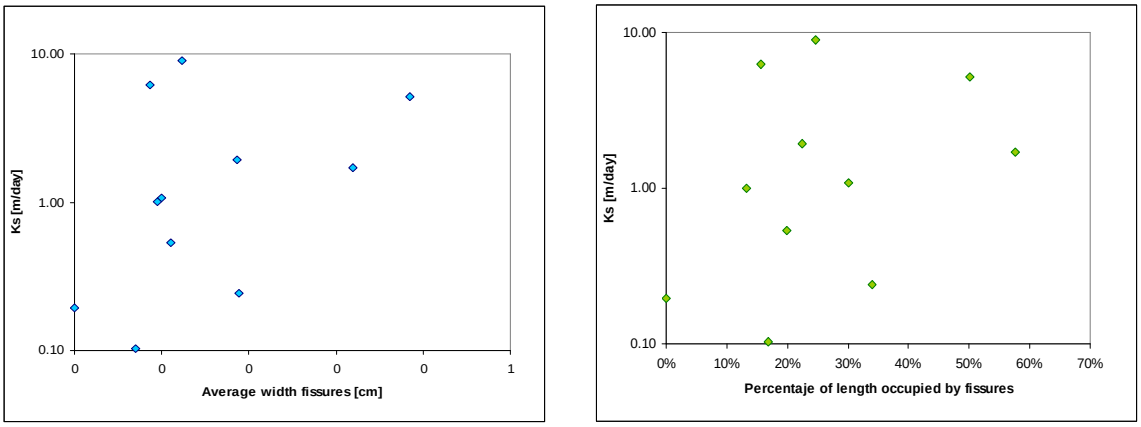

Figure 4.9 Ks vs. average fissure width and Ks vs. % open length

Finally, from the Ks analysis of different types of geomorphological units, it was found that Ks in the fissures varies within a small range in the crests and gullies areas. Ks in the matrix also varies within a small range in the crests, the upper part and the stable area. Conversely, large variation of Ks occurs on flows and landslides areas. These ranges are stated in table 4.8.

Table 4.8 Ks variation in types of geomorphological units

Geom. Unit	Fissures		Matrix	
	CV [-]	Range log Ks [m/day]	CV [-]	Range log Ks [m/day]
Crests	0.93	10^{0} – 10^{1}	1.03	10^{-2} – 10^{-1}
Landslides	1.21	10^{-2} – 10^{1}	1.97	10^{-3} – 10^{1}
Flow	1.71	10^{-3} – 10^{1}	1.97	10^{-3} – 10^{1}
Gullies	0.71	10^{-2} – 10^{-1}	1.76	10^{-3} – 10^{0}
Upper part	Only immediate drainage		0.65	10^{0} – 10^{1}
Stable	No fissures		1.37	10^{-3} – 10^{-2}

In the upper part of the landslide, immediate drainage occurred in all the tests in the fissures, whereas it occurred in more than 50% of the tests in the matrix. Furthermore, the measured values are very high, having a geometric mean of 15 m/day.

In the study of Malet et al., (2002), a relation between values of Ks in selected microplots with specific soil surface characteristics. Although the plots were

randomly selected, it was found that most of the plots of the same type are located on the same type of geomorphological units.

4.4.1. Probability density functions (PDF) in the fissures

The set of the calculated Ks in the fissures fits well with a log-normal function. Since the two factors that define the goodness of fit are accomplished: the function provides a good visual match and the results of the tests of fit provide low values.

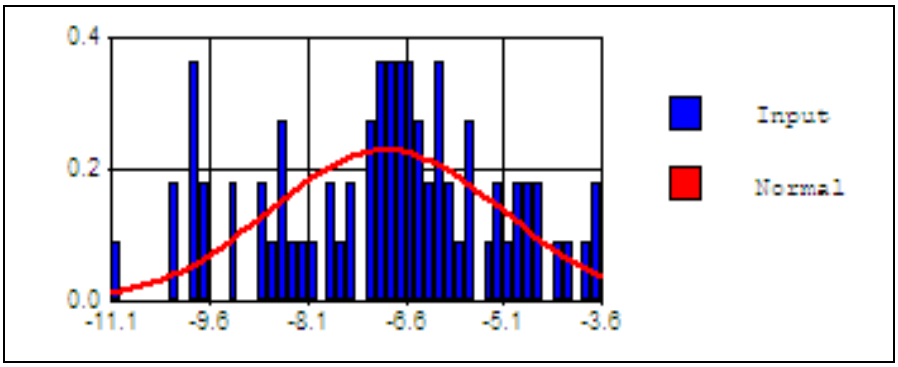

Figure 4.10 Normal distribution of Ln Ks in the fissures

The mean and the standard deviation of the probability density function of the natural logarithms of Ks in the fissures material are -6.91 and 1.77, respectively.

The probability of occurrence of preferential flow is calculated as indicated in section 3.5.

$$P(PF) = \frac{40}{114} = 0.35$$

In order to include the probability of preferential flow, the PDF is modified according with the theorem of total probability.

$$P(ln(Ks)) = \frac{1}{\sqrt{2\pi \times 1.77^2}} e^{\frac{-(\ln(Ks)+6.91)^2}{2\times 1.77^2}} \times 0.65$$

This equation applies to ln Ks smaller than -3.4, higher values have probabilities of 0.35.

Ks from flow areas also follow a log normal distribution with mean and standard deviation equal to -6.93 and 2.21. The probability of preferential flow in this area is 0.18 giving the following probability function.

$$P(ln(Ks)) = \frac{1}{\sqrt{2\pi \times 2.21^2}} e^{\frac{-(\ln(Ks)+6.93)^2}{2\times 2.21^2}} \times 0.82$$

There number of data in other type of units is too short to calculate probability density functions, hence only the probability of preferential flow was calculated.

Table 4.9 Probability of preferential flow in the fissures

Geom. Unit	Prob. PF
Flow	0.18
Landslides	0.32
Crests	0.64
Gullies	0.27

4.4.2. Probability density functions in the matrix

The data set in the matrix also follow a lognormal distribution. Given that the obtained function provides results of the three evaluated tests of fit very are near to zero, although not a very good visual match.

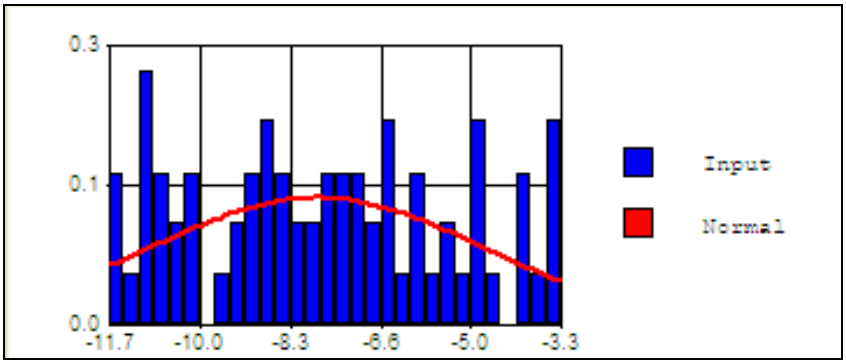

Figure 4.11 Normal distribution of Ln of Ks in matrix materials

The mean and the standard deviation of the probability density function of the natural logarithms in the matrix are -7.83 and 3.11, respectively. The probability of occurrence of preferential flow is 0.1.

The modified function including the probability of preferential flow is:

$$P(ln(Ks)) = \frac{1}{\sqrt{2\pi \times 3.11^2}} e^{\frac{-(\ln(Ks)+7.83)^2}{2\times 3.11^2}} \times 0.9$$

This equation apply to ln Ks lower than -3.6, higher values have probability of 0.1.

Although the log-normal distribution for the set of Ks from the flow areas gives good values of the tests of fit and is on the firsts positions on the rank done by the BEST-FIT software, the visual match is not good, being more similar to a double peak distribution. Thus, the set of data does not follow a log-normal distribution or any of the other evaluated functions.

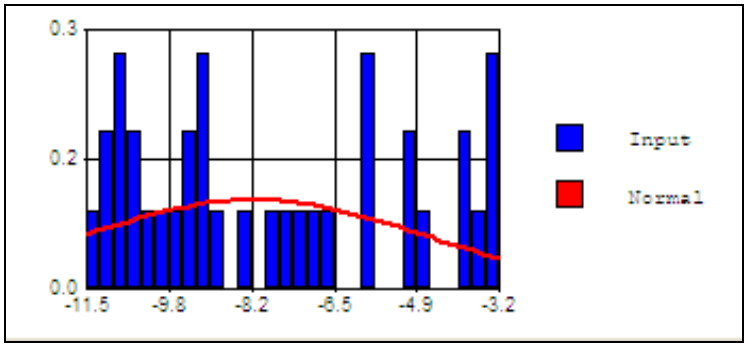

Figure 4.12 Normal distribution of Ln of Ks in the flow areas

The probability of preferential flow in the different types of geomorphological units was calculated as follows.

Table 4.10 Probability of preferential flow in the matrix

Geom. Unit	Prob. PF
Flow	0.07
Upper	0.56

4.5. ANALYSIS OF SPRINKLER TESTS

In this section, the preferential flow is calculated in any of the three sprinkler experiments, mentioned in section 3.4. First the set-up of the tests and the collected information are described, and then the water balance and the preferential flow are calculated.

4.5.1. Plot A. Reworked marls in weathering process

4.5.1.1. Description of the plot and experiment set up

Plot A is located immediately below the main scarp of the landslide. It is the uppermost of the three analyzed plots. The place corresponds to the type unsealed clasts with reworked of marls in weathering process varying in dipping as described by Malet (2002). The plot is located on the upper part of the landslide, according with the geomorphological classification.

Marly blocks of nearly 2 cm are observed on the surface of the rained-on plot, as well as almost-filled fissures of about 10 cm width. On both days of the experiments, 14 periods of 15 minutes of rain were applied, whereas an additional rainfall of 45 minutes was applied at the end of the experiment on the second day. The intensity of the rainfall was maintained at an almost constant rate. The amount of applied rain is shown in table 4.11.

Table 4.11 Applied rainfall in plot A

	Number of rain events	Intensity (mm/min)	Avg. rain per event (mm/15min)	Total rain (mm/7 hours)
Day 1	14	1.29	19.42	272
Day 2	15	1.30	19.54	332

The plan view and the profile of the experiment set up are shown in figure 4.13.

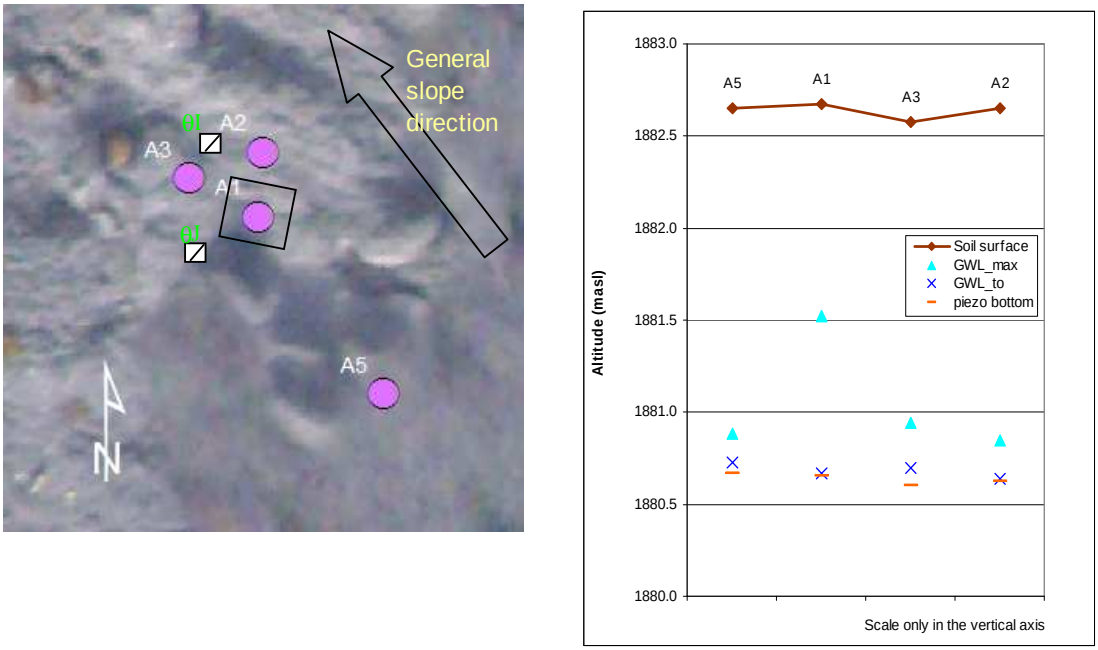

Figure 4.13 Experimental set up Plot A

4.5.1.2. Hydraulic head responses and soil moisture content

The groundwater table before the experiment was found at the same level of the bottom of the piezometers that were at depths of 2 m.

The applied rain created negative hydraulic gradients between the plot and the sides. Maximum increases of water level were 0.9 m at the center of the rained-on plot, 0.2 m in the surrounding piezometers A2 and A3 and, 0.1 m in A5; no change was observed in A7.

Fluctuations of the GWL of 0.25 m on every rainfall block were measured in A1 on both days of the experiment (figure 4.14). The drawdown lasted four hours.

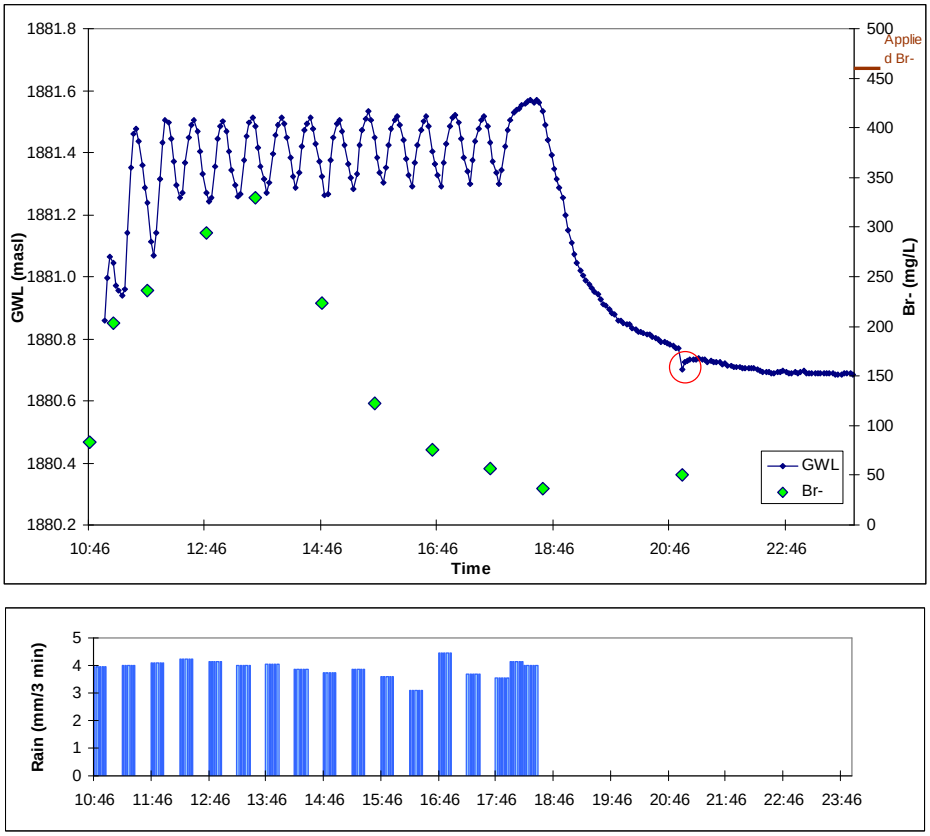

Figure 4.14 Groundwater level and tracer response – Piezometer A1, day 2

Although a response was registered in A5, it is not considered that flow occurred towards this piezometer because no tracer was found there. Then, the flow lines are defined with the hydraulic heads on piezometers A1, A2 and A3 as is illustrated in figure 4.15.

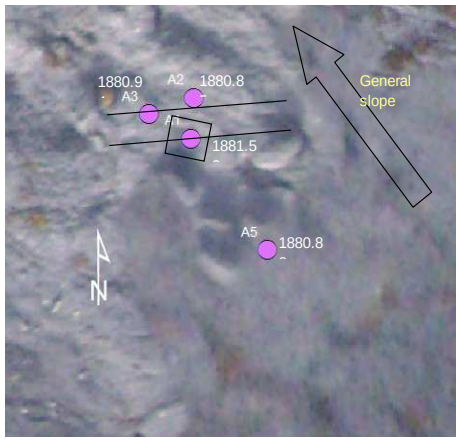

Figure 4.15 Flow lines from maximum water levels in Plot A

The soil moisture content in the plot changed between 0.6 and 1 m on the theta probe rods located in the direction of A2 and A3, from 20% to 60%. No change was registered in the other rod. The plots of soil moisture measurements are in appendix V.

4.5.1.3. Tracers analysis

The rain applied on the first day had a concentration of 118 mg/L of Br^-. The tracer was found in piezometer A1 from the first rain event. Its concentration increased with time, until a maximum of 99 mg/L after the last rain. Concentrations of Br^- lower than 50 mg/L were found on A2 and A3, but none in A5. On the second day, Br^- was applied during the first 4 rain blocks with a concentration of 461 mg/L. Maximum concentrations were registered one hour later of the fourth rain in A1, after 2 hours in A2 and after 3 hours in A3.

Table 4.12 Bromide concentration in plot A

Location	Day 1	Day 2
	Max Br^- conc. (mg/L)	
Rain	118	461
GW	0	0
A1	99	329.7
A2	44.9	186.0
A3	31.2	160.2
A5	0.0	0.0

4.5.1.4. Water balance

No overland flow or exfiltration occurred in the plot. Thus, the components of the water balance are the applied rain, the subsurface flow out of the plot and the change in storage.
The water balance was calculated only on day 2 because the time series of GWL missed the initial and final part of the experiment. Porosity varies in the area from 0.32 to 0.35 and initial soil moisture is taken as 0.2. Specific yield was calculated as 0.07. The cumulative storage at the end of the last rain obtained from the water balance was 0.095 m^3. Whereas this storage calculated from the porosity values varied between 0.108 and 0.135. The percentage difference is 15% to 43%. The resulting components of the water balance on daily basis are:

Table 4.13 Water balance in plot A - day 2

Component	Value
P (m^3/8 hr)	0.332
SSF(m^3/8 hr)	0.239 - 0.251
$\Delta S / \Delta t$ (m^3/8 hr)	0.081 - 0.093

4.5.1.5. Quantification of preferential flow

The drawdown curve of piezometer A1 on day 2 is used to identify the volumes of fast and slow drainage. Two storages are identified from the inflexion point which is observed after 2 hours to the end of the rain (Figure 4.16). The volume calculated from the steepest part of the curve represents the fast drainage and the other, the matrix-like flow. The recession constants were calculated as 55 minutes for the fast drainage and 95 minutes for the slower.

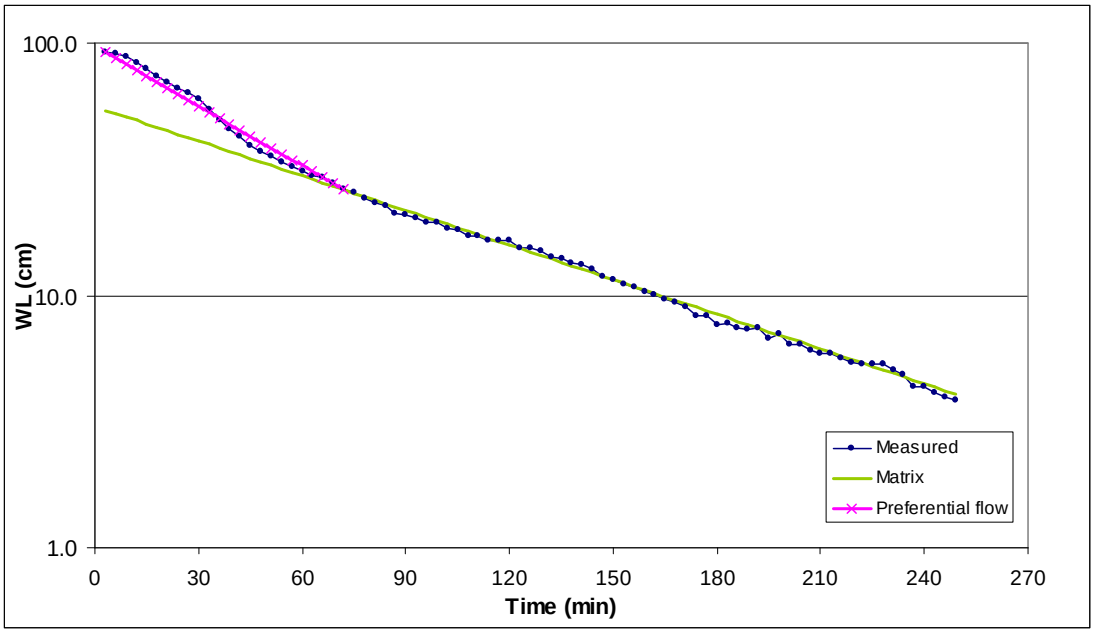

Figure 4.16 Drawdown curve A1 – Day 2

The Darcy's flow was calculated from the heads from the recession curve correspondent to matrix flow. Hydraulic gradients were calculated from the flow lines showed in figure 4.14. Ks was taken as the geometric mean of the upper part of the landslide equal to 11.5 m/day.

The cumulative matrix flow from the recession is calculated as 0.051 m^3. The ratio matrix flow - total flow during the recession is 0.54, and then the preferential flow is equal to 0.56 of the total flow.

4.5.1.6. Hydrological conceptualization of plot A

The infiltration rate of the plot is higher than the intensity of the applied rain of 40 mm/hr. There is an important amount of pre-event water which dilutes the artificial rain.

High response in water table is registered in the piezometer located in the center while very limited in the lateral ones, indicating that vertical groundwater recharge is dominant in the plot.

Fast drainage occurs, since the drawdown lasted 4 hours. Hence preferential and matrix flow are rapid, even though the preferential flow is twice as fast as the matrix flow, as indicated by their values of K . The preferential flow is estimated as 56% of the total flow during the drawdown.

4.5.2. Plot B. Stable area

4.5.2.1. Description of the plot and experiment set up

Plot B is located in the most stable part of the landslide, i.e. the area with smaller displacements. There are dense black marls with big stones in the surface and no fissures are observed. The soil unit in this area according to Malet (2002) is the type depositional crusts with clayey–silty texture.

On both days of the experiment, 14 rain fall periods were applied, varying from 10 to 15 minutes each, separated by 15 minutes of no rain. The characteristics of the applied rain are shown in table 4.14.

Table 4.14 Applied rainfall in plot B

	Number of rain events (-)	Intensity (mm/min)	Avg. rain per event (mm/15 min)	Total rain (mm/8 hr)
Day 1	14	1.29	20.8	291
Day 2	14	1.30	21.7	304

The plan view and the profile of the experiment set up are shown in figure 4.17.

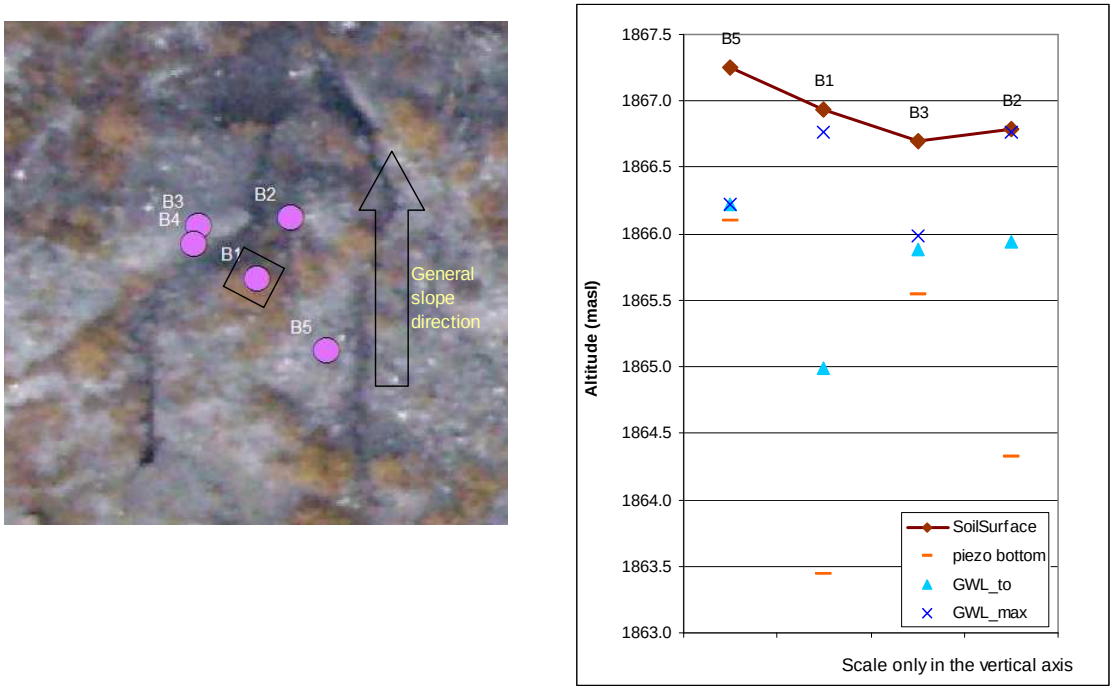

Figure 4.17 Plan view and profile plot B

4.5.2.2. Hydraulic head responses

Four piezometers were installed in the area of the experiment as shown in the previous figure. The piezometers were installed at various depths from 1.30 to 3 m, since it was not possible to reach the same depths due to the presence of rocks. The groundwater level was two meters deep on piezometer B1 whereas it is around 85 cm on the surrounding piezometers B2 and B3.

In response to the applied rain, a maximum increase of the groundwater level was measured at B1 to be 1.7 m with fluctuations of 0.25 m for every 15 minute rainfall event. The dropdown stopped after 4 hours; from that moment the water table remained constant at 0.75 m from the soil surface on both days of the experiment. For further calculations this level is taken as the original water level in B1.

At piezometer B2, the maximum increase of the groundwater level was 0.75 m and the fluctuations due to any rain were 0.20 m. The groundwater level decreased over 12 hours after the end of the experiment until it reached a depth of 0.8 m below the soil surface. There was no response in piezometers B3 and B5.

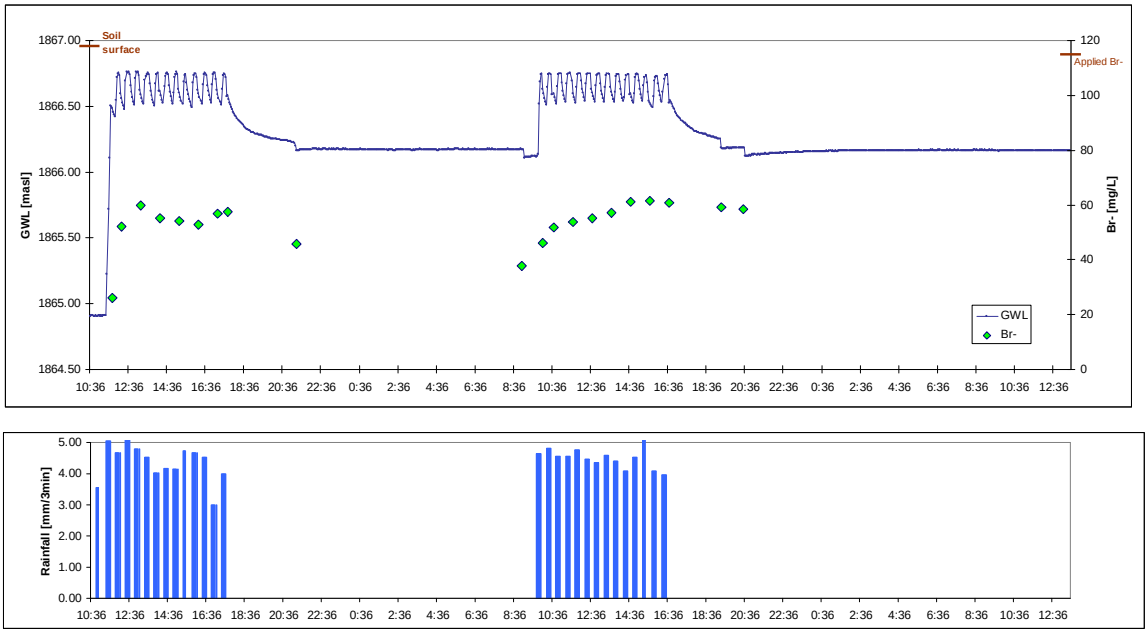

Figure 4.18 Groundwater levels and tracer response – Piezometer B1

4.5.2.3. Tracers analysis

The applied rain during the first day had a concentration of 115 mg/L of Br^-. In A1 the concentration of Br^- remained relatively constant after the fourth rainfall period during the first day and was maintained during the second day when no tracer was applied. On the other hand, the electrical conductivity in B1 before the experiment was on the order of 6300 µS/cm but only about 4000 µS/cm in B2.

In B2 a maximum concentration of 35 mg/L was registered after the last rain on the first day; it increased until 50 mg/L on the second day. In B3 concentrations lower than 1 mg/L were found whereas no tracer was found on B5.

4.5.2.4. Water balance

An important component of the water balance in plot B is overland flow which amounts to 73% of the applied rain on day 1 and 74% on day 2. Consequently, ponding occurred in the whole area of the plot.

The components of the water balance are the applied rain, the overland flow, the subsurface flow towards B2 and the change in storage. In plot B, was found that saturation very likely occur in an area smaller than one square meter, since a very small porosity would be required to cause the measured increase in the water level with the infiltrated volume. In consequence, the saturated area was iterated along with the specific yield.

The water balance was calculated using values of porosity from 0.32 to 0.35 and an initial water content of 0.2; this value was measured in the stable area during the field work. Specific yield was found equal to 0.02. The values of cumulative storage at the end of the last rain obtained by the two calculation methods mentioned in the methodology, the calculated saturated area and the percentage error are shown in table 4.15.

Table 4.15 Water balance parameters in plot B

Parameter	Day 1	Day 2
Saturated area (m^2)	0.65 – 0.70	0.6 – 0.65
Sy (-)	0.02	0.02
S t=end – from WB (m^3)	0.013 – 0.014	0.006 – 0.008
S t=end – from porosity (m^3)	0.014 – 0.016	0.005 – 0.006
Difference (%)	2 -21	20 – 28

The calculated components of the water balance are:

Table 4.16 Water balance plot B

Component	Day 1	Day 2
P (m^3/7 hr)	0.291	0.304
OLF (m^3/7 hr)	0.211	0.226
SSF (m^3/7 hr)	0.074 - 0.075	0.073 - 0.075
$\Delta S/\Delta t$ (m^3/7 hr)	0.005 - 0.006	0.003 – 0.006

4.5.2.5. Quantification of preferential flow

In B1 the drawdown stopped after 4 hours of the end of the rain whereas in B2 fast decrease was observed during the six hours after the stop of the rain, followed by a slower decrease which lasted 24 hr.

Although no fissures are observed in the area, some macropores exist, causing very fast responses in hydraulic head and fast drainage. Two storage types are identified from the drawdown curve, one being the very fast drainage and the other the matrix-like flow.

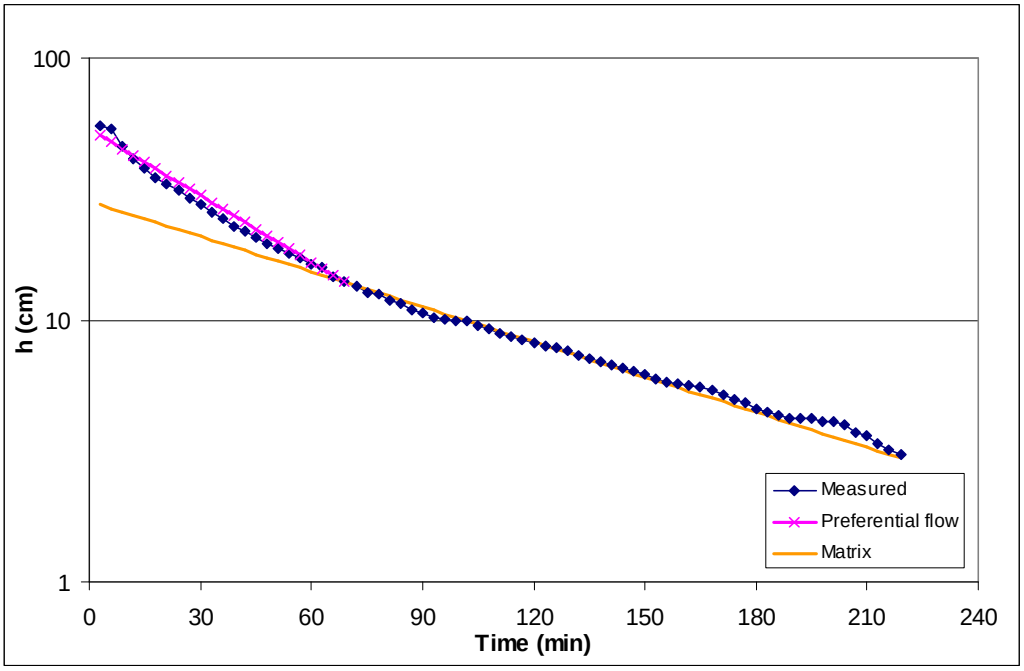

Figure 4.19 Drawdown curve piezometer B1 day 1

The calculated recession constants K1 for the fast drainage system and K2 for the slower are shown in table 4.17.

Table 4.17 Recession constants in Plot B

Recession constant	B1		B2
	Day 1	Day 2	Day 1
K1 (min)	51	26	50
K2 (min)	97	64	240

It was not possible to calculate the Darcy's flow between B1 and B2 because the measured GWL in B2 is some millimeters higher than in B1.

4.5.2.6. Hydrological conceptualization of plot B

The matrix in Plot B had the lowest Ks of three test sites. Here, most of the applied rain constituted overland flow, which was almost 75% of the applied rain on both days. Ponding was observed during the entire experiment in the rained area showing that the infiltration rate is lower than 15 mm/hr. However, the small infiltrated volume caused very high increases of the water level on piezometers B1 and B2.

The lower groundwater level in the center of the plot seems to be due to lower hydraulic conductivity in the deeper materials. It is observed from the higher value of EC in the piezometer B1 than in piezometer B2 which is one meter shallower than the first one. This difference in EC may indicate that in the deeper level, water had a longer travel time that allowed its ionic enrichment. This premise can be supported by the presence of Br^- in B1 on the second day when it was not applied. Local differences in soil materials are also shown by the big difference of the calculated recession constants of the matrix on piezometers B1 and B2.

The calculations from the water balance indicate that saturation occurred in part of the rained plot. This can be due to local differences in materials having poor hydraulic connectivity which also explained the absence of response in other piezometers located next to the plot. This area was estimated from the calculation of the water balance as 0.3 to 0.5 m^2. However this water balance has high uncertainty due to the small infiltrated volume used to its calculation, the need of iterate the saturated area and the existence of differences in hydraulic properties in depth.

4.5.3. Plot C. Mudslide deposit

4.5.3.1. Description of the plot and experiment set up

Plot C is located in a deposit area, characterized by very dynamic behaviour. Some fissures of about 10 cm width and partially filled were located across the plot. The type of soil in the plot is gravel crust characterized by coarse fragments, bigger than 2 mm embedded in a crust of 3.5 to 4 cm depth, overlapping a finer matrix, according with the soil characteristic units defined by Malet (2002).

On both days of the experiment, 14 periods of 15 minutes of rain were applied, whereas an additional rainfall of 45 minutes was applied at the end of the experiment on the second day. The characteristics of the applied rain are shown in table 4.18.

Table 4.18 Applied rain characteristics in Plot C

	Number of rain events (-)	Intensity (mm/min)	Avg. rain per event (mm/15 min)	Total rain (mm/ 8 hr)
Day 1	14	1.73	26.0	364
Day 2	15	1.64	24.6	419

Four piezometers and two theta probes were installed in Plot C as shown in the plan view and the profile on figure 4.20.

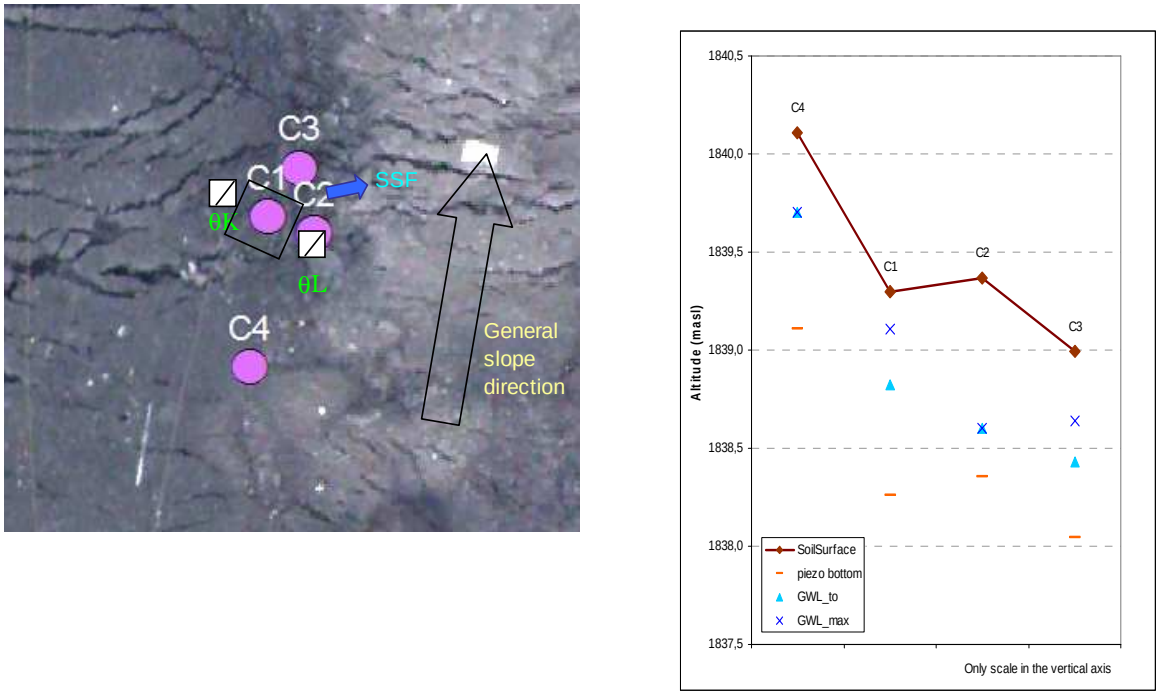

Figure 4.20 Experiment set up Plot C

4.5.3.2. Hydraulic pressure responses

The groundwater table before the experiment is near 0.5 m from the soil surface. The piezometric levels indicate that the groundwater flow occurred in the direction C4 to C3 before the experiment. The groundwater flow above the bottom of the piezometer C1 was calculated as $2.1X10^{-06}$ m^3/s, with Ks equal to 3.9 m/day. During the experiments the gradients are changed but the direction of the flow stayed the same.

Maximum increases of about 0.25 m were measured in piezometer C1 and of 0.20 m in C3. Responses in groundwater level were observed only in these

piezometers. Fluctuations of 0.06 m occurred on C1 on every 15 minutes rain event and of 0.08 m in C3. The drawdown in both piezometers lasted more that 17 hours.

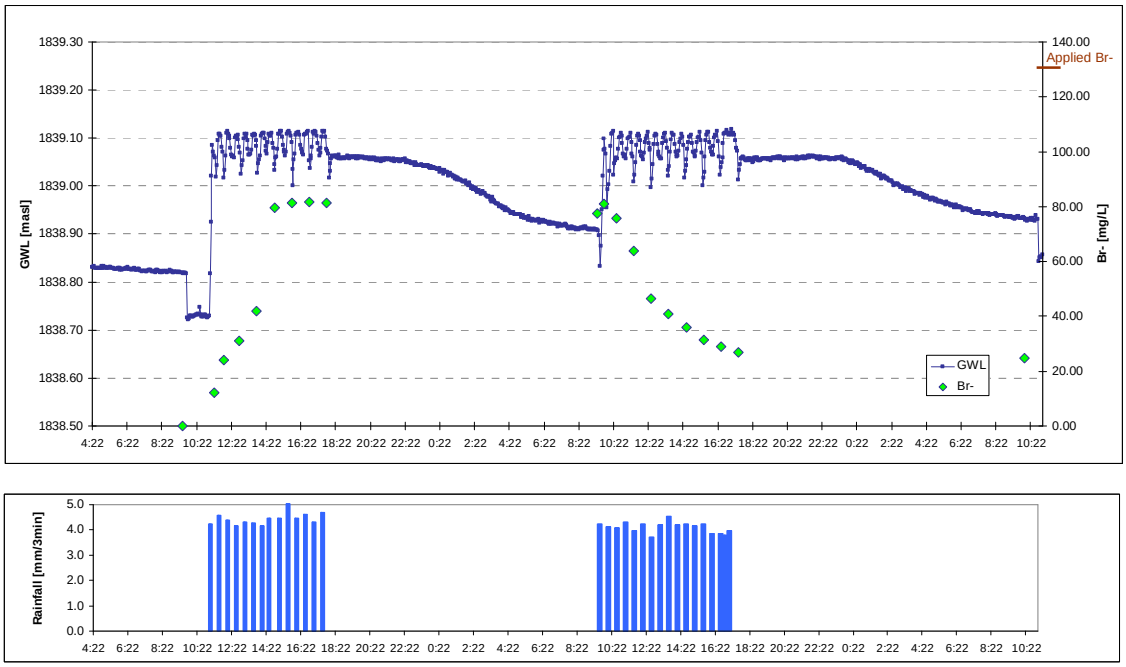

Figure 4.21 Groundwater levels and tracer response – Piezometer C1

4.5.3.3. Tracer's analysis

Cl^- and Br^- showed similar behaviour with significant increases in C1 and higher concentrations in C3. In the exfiltration flow, the concentration of both tracers was the same as the applied in the rain.

Br^- was found in C1 after the first rain event; the concentration increased until the eighth rainfall and remained relatively constant afterwards. The tracer was also found in A3 from the first sample. The measured concentrations are shown in table 4.19.

Table 4.19 Tracer's response in plot C - day 1

Location	**Max conc,** Br^- **(mg/L)**	**Max conc.** Br^- **(mg/L)**
Rain	125	130
GW	0	7
C1	80	74
C3	110	120
Exfiltration	125	130

4.5.3.4. Water balance

No overland flow occurred during the two days of experiment on plot C. Surface outflow occurred near the lowest vertex of the plot after the fourth rain on day 1 and from the first rain on day 2. This vertex was located at the same face of the plot than piezometer C3, as illustrated in figure 4.19. On the first day of experiment the exfiltration amounted 50% of the applied rain whereas it was 70% on the second day.

The main components of the water balance in C1 are the applied rain, the vertical flow towards C1, the subsurface flow to C3 and the surface outflow.

The values of porosity of 0.38 to 0.40 were used for the water balance calculation; the initial water content was 0.25. The values of specific yield, cumulative storage at the end of the last rain obtained by the two calculation methods mentioned in the methodology and the percentage error are shown in table 4.20.

Table 4.20 Water balance parameters in plot C

Parameter	**Day 1**	**Day 2**
Sy 1 (-)	0.2 - 0.21	0.18
Sy 2 (-)	0.13 - 0.14	0.09 - 0.10
S t=end – from WB (m^3)	0.047 - 0.048	0.096
S t=end – from porosity (m^3)	0.038 – 0.044	0.076 - 0.080
Difference (%)	8 - 20	16 - 21

It is worth to notice that two different values of Sy had to be used in order to obtain similar values of storage by the two methods of calculation, and at the same time to obtain a cumulative change of storage near to zero. Sy 1 was used for the period of the artificial rain while Sy 2 to the drawdown curve after the rain had stopped. The calculated components of the water balance are:

Table 4.21 Water balance plot C

Component	Value - Day 1	Value - Day 2
P (m^3/8 hr)	0.364	0.419
SSF (m^3/8 hr)	0.344 – 0.348	0.411 – 0.413
$\Delta S/\Delta t$ (m^3/8 hr)	0.016 - 0.018	0.006 – 0.008

4.5.3.5. Quantification of preferential flow

The drawdown in C1 was measured during 16 hours on the first day; in this period the water level decreased until 10 cm above the original water level. On

the second day, the drawdown lasted 17 hours (Figure 4.22). An inflexion point occurred 21 minutes after the end of the rain on both days.

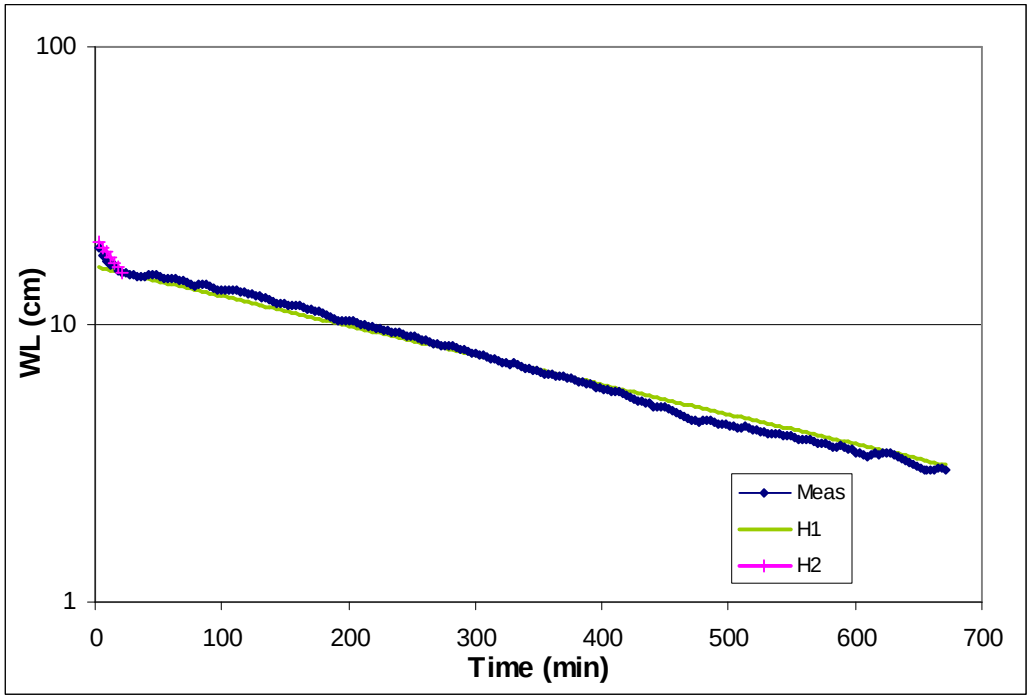

Figure 4.22 Drawdown curve C1 – Day 2

The calculated recession constants K1 for the fast drainage system and K2 for the slower are shown in table 4.22.

Table 4.22 Recession constants in Plot C

Recession constant	Day 1	Day 2
K1 (min)	48	72
K2 (min)	390	408

Darcy's flow during the experiment was calculated from plot C using the changes in groundwater level from the curve correspondent to matrix flow. Hydraulic gradients are calculated between C1 and C3. The flow out of the plot is calculated as occurring through an area of 1 m width and the height of water in C1 at any time step.

The total matrix flow during the drawdown is equal to 0.027 m^3 on the first day and 0.026 m^3 on the second day. The calculated matrix flow during the first 15 minutes of the drawdown was used to estimate the total matrix flow during the rain period. Since the water level during this period is the same than in the

previous rain blocks. The estimation of the total matrix flow and the ratio matrix flow/total flow is included in table 4.23.

Table 4.23 Calculation of matrix flow

Day	Drainage 15 min (m^3)	Duration of rain (hr)	Matrix flow on the rain period (m^3/8 hr)	Total matrix flow (m^3/24 hr)	Matrix flow / Total flow
1	0.0019	6:45	0.0513	0.0784	0.23
2	0.0018	7:45	0.0558	0.0818	0.20

4.5.3.6. Hydrological conceptualization of plot C

Plot C is characterized by a higher infiltration rate than the applied rain, i.e. 52 mm/hr, in fissures and matrix materials. Rapid vertical and downslope flow occurred. In contrast, no lateral flow was observed, since it was no response in piezometer C2 or changes in soil moisture content during or after the experiments.

From the drawdown curve it is observed that the preferential flow occurred in a short time, i.e. on the 21 minutes after the end of the rain, from when a marked change in the slope of the drawdown curve is identified.

The preferential flow is calculated as 77 to 80% of the total flow. This flow includes part of the subsurface flow towards C3 and the exfiltration flow, since higher concentration of Br^- were found in these flows than in C1, indicating that part of the infiltrated water was not mixed with the groundwater in C1.

4.5.4. Discussion of results

The three plots of sprinkler test showed markedly different hydraulic behaviour. Plots A and C have very high infiltration capacity whereas it was very low in plot B. Another important difference is the time for drainage which was 4 hours in plot A, between 4 to 17 hours in plot B and near 24 hours in plot C. the summary of the hydrological descriptors of the plots are in the following table (Table 4.24)

Table 4.24 Hydrological properties of the sprinkler tests sites

Plot	Inf. capacity (mm/hr)	Drainage time (hr)	Pref flow / Total flow	K (min)	
				Matrix	Fast
A	40	4	0.56	55	95
B	<15	4-17	NC	50 - 51	97 - 240
C	54	24	0.80	48 - 72	390 - 408

Ks in the area of plot A is the highest of the three locations, it was found there that immediate drainage occurred in all the auger hole test in the fissure materials. This might be the main cause of the vertical flow, which was identified by the limited response on the piezometers around the plot. The drainage in this area was the fastest of all the plots. The recession constant from the slow drainage is double of the constant from the fast drainage. So both preferential and matrix flow are very fast. The fast drainage in plot A limits the effect on the instability of the slope since the excess of porewater pressure is dissipated on very short periods of time. The importance of this area for the instability of the underneath slopes might be caused by the high infiltration capacity which feed the groundwater system in the upper part of the landslide.

Plot B had the lowest Ks in the matrix and no identifiable fissures in the surface. The infiltration capacity is very low, since near 75% of the applied rain represent overland flow. The area is understood as formed by heterogeneous materials with small hydraulic connectivity since increases of water level occurred only at two piezometers. Moreover, the time of drainage in these two piezometers had significant differences. Instability would occur by the increase in pore water pressure when prolonged rainfalls occur.

Plot C was located on the most dynamic part of the landslide. It had very shallow groundwater level which increased rapidly with the artificial rain. All the applied rain was infiltrated but more than 50% flowed out at the surface, downslope of the plot. The higher concentration of tracer found in this flow and in piezometer C3 than in the center of the plot, reveals that rapid flow occur towards these locations, without being mixed with the groundwater in C1. The preferential flow in plot C amounts 80% of the total flow.Part of the flow drained rapidly but other part slower, maintaining the groundwater level elevated. The time of drainage of this slow drainage is more than five times than the fast one.

The relation of the hydrological behavior and the stability on the sprinkled plots is represented in the following graph.

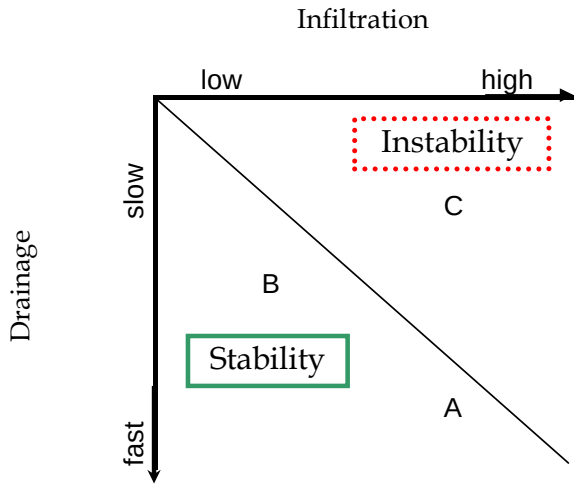

Figure 4.23 Hydrological characteristics and stability of the sprinkler tests sites

For the definition of areas with similar hydrological characteristics, it was found that the upper part of the landslide (3.fd), near to the main scarp has very high infiltration capacity. High values of Ks and high probability of preferential flow are characteristic of this area.

In the rest of the areas, Ks can be defined by the probability density functions derived in the section 4.4 for the matrix and the fissures. The following map shows the proportion of the area covered by fissures on different locations within the landslide. The locations with bigger surface covered by fissures will have higher Ks as well as higher probability of preferential flow.

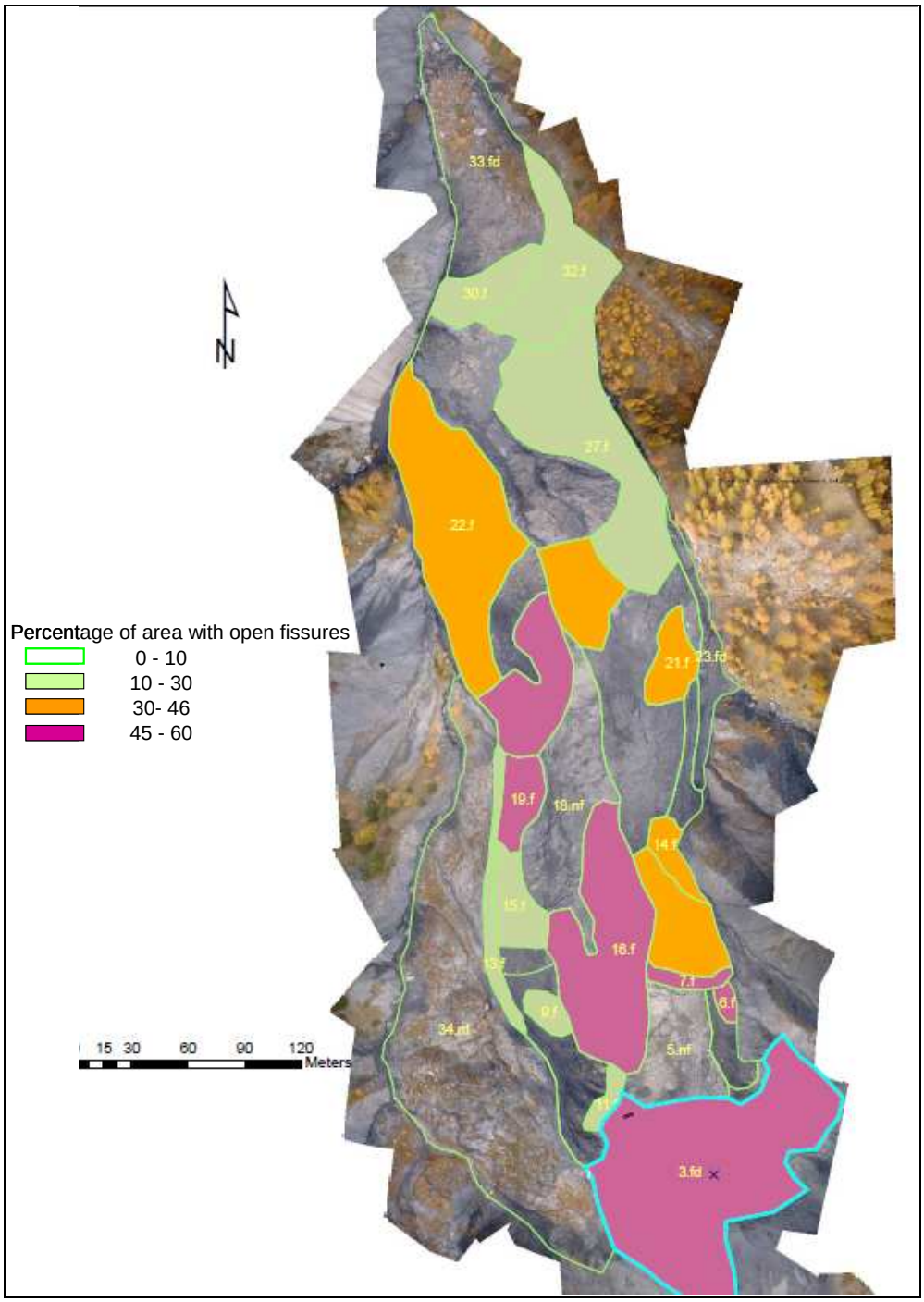

Figure 4.24 Classification of areas with fissures

5. CONCLUSIONS AND RECOMMENDATIONS

A lack of correlation of the geomorphological descriptors with Ks was found. This can be due to the great variability of Ks that occurs even within specific areas, or because the individual geomorphological characteristics do not represent the characteristics of the soils that affect this parameter.

Areas with fissures deeper than one meter and wider than 0.3 m were found in the crest areas and in the crowns of some earthflows, in these locations the fissures cover more than 50% of the surface. In these areas the infiltration rates must be significantly higher than in the soil matrix due to the presence of fissures.

The log-normal functions defined for the matrix and for the fissures are advisable to be used in order to assign Ks values to different locations within the landslide. However, it was identified that in some types of geomorphological areas, as the crests and gullies, Ks varies in small ranges and they differ in the probability of preferential flow. Thus, different probability functions could represent better the variation of Ks in these specific locations.

Preferential flow can be initiated directly on the fissures, especially in those areas with wide and deep fissures, i.e. wider than 0.2 m and deeper than 1 m, cover a high percentage of the surface. In contrast, in the narrow fissures, the flow is expected to initiate only after overland flow occurs.

The analysis of the drawdown curves allows the identification of different kinds of storages, although some uncertainty comes from the calculation of drained volumes by the changes in head. Sprinkler experiments with instantaneous application of conservative tracers, similar to the ones cited in the literature review (Maloszewski et al, 2006; Weiler & Naef, unpublished; and Stumpp et al. 2007), can be helpful to model hydraulic properties of the preferential and matrix flow. These parameters were obtained by the analysis of breakthrough curves from locations that were representative of flow by the matrix and by the fissures.

The upper part, near to the main scarp of the landslide was found to have very high infiltration capacity as well as very fast drainage; these conditions together are not critical for instability. However, the high infiltration capacity of the area can play an important role in the groundwater recharge toward downslope sites.

On the other hand, the reduced infiltration on the stable area does not create an important excess of pore pressure, the time of drainage in this area had big

variation between the two analyzed piezometers. Finally, the most dynamic part of the landslide has the most unfavorable conditions to create instability, high infiltration capacity and long time of drainage. 80% of flow was identified to be faster that the matrix flow.

For the definition of hydrological response units for modeling, it is advised to differentiate the upper part of the landslide as well as the central crest as sites with high infiltration capacity.

6. REFERENCES

Bear, Jacob. Dynamics of fluids in porous media. 1972.

Beven, K. J. & Germann, P. F. Macropores and water flow in soils. *Wat. Resour. Res.* 18(5), 1311-1325. 1982.

Bogaard, T. Analysis of hydrological processes in unstable clayey slopes. Utrecht University. 2001.

Bromhead, N. E. The stability of slopes. Surrey University Press. 1986

de Laat, P., Savenije, H. Hydrolgy. Lecture notes, UNESCO-IHE. 2006.

Foppen, J.W., Nonner, J., Beevers, L. Hydrogeological fieldwork Digne les Bains – Field manual. UNESCO-IHE. 2008.

Kirkby, M.J. Hillslope hydrology.John Wiley & Sons. 1978

Kreft, A; Zuber, A. On the physical meaning of the dispersion equation and its solutions for different initial and boundary conditions. Chem. Eng. Sci. Vol 33. 1978.

Krzeminska, D. Quantitative analysis of preferential flow during small scale infiltration tests on an active mudslide, French Alps. 2009. Non published

Linsley, R.K., Kohler, M.A., Paulhus, J.L. Hydrology for engineers. McGraw-Hill Book Company. 1982.

Malet, J. Les 'glissements de type écoulement' dans les marnes noires des Alpes du Sud. Morphologie, fonctionnement et modélisation hydro-mécanique. Université Louis Pasteur. 2003.

Malet, J., Auzet, A., Maquaire, O., Ambroise, B., Descroix, L. Soil surface characteristics influence on infiltration in black marls: application to the Super-Sauze earthflow (Southern Alps, France) in Earth surface processes and landforms 28, 547-564. 2003.

Malet, J., van Asch, T., van Beek, R., Maquaire, O. Forecasting the behaviour of complex landslides with a spatially distributed hydrological model. in Natural Hazards and earth System Sciences 5., 71-85. 2005.

Maloszewski, P., Wachniew, P., Czuprynski, P. Polish Journal of Environmental studies Vol. 15, No. 1. 106-110. 2006

Mikovari, A., Peter, C., Leibundgut, Ch. Investigation of preferential flow using tracer techniques. Department of Hydrology, University of Freiburg. Tracer Technologies for Hydrological Systems (Proceedings of a Boulder Symposium, July 1995). IAHS Publ.no. 229, 1995.

Niethammer, U., Rothmund S., Joswig M. UAV-based remote sensing of the slow moving landslide Super-Sauze. In Malet J.P., Remaitre, A., Bogaard, T. Landslide Processes: From geomorphologic mapping to dynamic modelling. 69-80. CERG Editions. France. 2009.

Nwaiwu C. Statistical Distributions of Hydraulic Conductivityfrom Reliability Analysis Data, Geotech Geol Eng (2009) 27:169–179

Nonner, J.C., Introduction to hydrogeology. UNESCO-IHE lecture notes series. 2006.

Stumpp, C., Maloszewski, P., Stichler, W., Maciejewski, S. Quantification of the heterogeneity of the unsaturated zone based on environmental deuterium observed in lysimeter experiments. Hydrological sciences. 52, 748-762. 2007

Scanlon, T.M., Raffensperger, J.P., Hornberger, G.M. Shallow subsurface storm flow in a forested headwater catchment: Observations and modeling using a modified TOPMODEL. Department of Environmental Sciences, University of Virginia, Charlottesville. Water resources research, Vol. 36, No. 9, 2575–2586. 2000.

Van Westen, C.J., Van Asch, T., Soeters, R. Landslide hazard and risk zonation – Why is it still so difficult? *in* Bulletin of Engineering Geology and the Environment. 2005

Weiler M.H. Mechanism controlling macropore flow during infiltration. Swiss federal Institute of technology Zurich. 2001.

Weiler, M., Naef, F. An experimental study of the role of macropores in infiltration in grassland soils. Hydrol. Process. 17, 477-493. 2003

Weiler M. Naef, F. Study of runoff generation on hillslopes using tracer experiments and a phisically based numerical hillslope model. Unpublished.

Zeleke, T.B. and Cheng Si B. Scaling Relationships between Saturated Hydraulic Conductivity and Soil Physical Properties. Soil Sci. Soc. Am. J. 69. 2005

Appendix I. Location of rain gauges in sprinkler plots

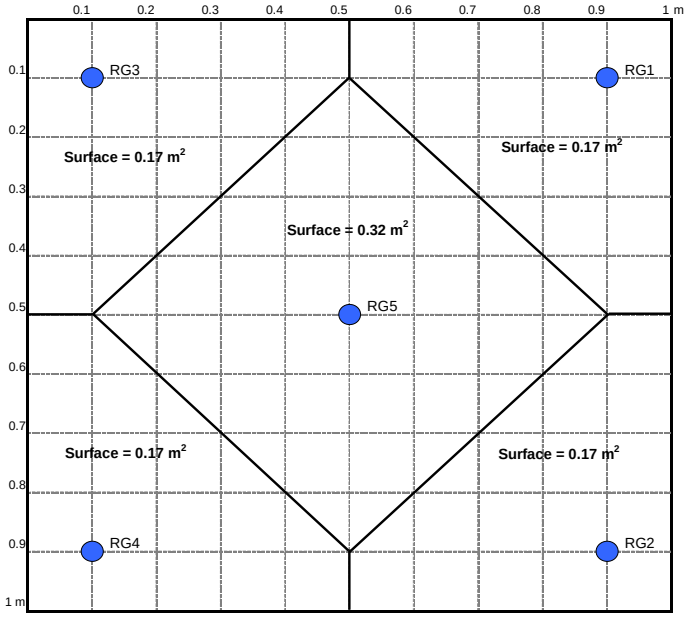

Appendix II. Numeric and classified geomorphological descriptors

FISSURES

FIELD_ID	NEW_ID	%_ROCK _COV	SIZE_ (cm)	SLOPE_ ANGLE	SLP_ TYPE	DENS_ #/5m	Width (m)	Depth (m)	Open_ Depth (m)	%Open _ length	Bulk density
01	30.f	0.35	5.00	20.00	convex	7	0.19	0.73		27%	
02	29.f	0.35	5.00	20.00	convex	7	0.19	0.73	0.00	27%	
03	8.f	0.40	5.00	20.00	convex	10	0.12	0.45	0.30	25%	1.814
04	11.f	0.70	5.00	45.00		5	0.24	1.32	0.67	24%	
05	3.fd	0.90	10.00	35.00	planar	8	0.03	0.26	0.05	5%	1.424
07	1.f	0.20	3.00	20.00	convex	8	0.07	0.76	0.00	11%	1.493
08	2.nf										
09	5.nf		6.00								1.494
11	14.f	0.80	3.00	20.00	convex	8	0.20	0.73	0.36	32%	
12	16.f	1.00	15.00	25.00		7	0.39	1.10	0.57	50%	1.551
13	10.f	0.80	10.00	30.00		6	0.18	0.84	0.42	22%	1.832
14	15.f	0.10	5.00	20.00	planar	6	0.19	1.00	0.43	22%	1.865
15	9.f	0.30	3.00	22.00		15	0.10	0.79	0.41	30%	
16	13.f	0.50	5.00	30.00		9	0.11	0.58	0.57	20%	
17	17.f	0.25	4.00			7	0.10	0.87	0.56	13%	1.516
17.5	18.nf	0.20					0.00			0%	1.834
18	19.f	0.70	15.00	10.00	radial	8	0.34	1.52	0.81	55%	1.726
19	23.fd	0.40	10.00				0.00	0.05	0.05	0%	1.824
20	21.f	0.40	5.00	15.00	planar	9	0.19	1.14	0.54	34%	1.761
21	20.f						0.00	0.00	0.00	0%	
22	24.nf	0.30		25.00	planar		0.00			0%	1.451
23	25.f	0.25	10.00			9	0.14	1.35	0.77	25%	
24	26.f	0.80	10.00			9	0.22	0.81	0.27	40%	
25	27.f	0.50	20.00		planar	9	0.09	0.90	0.34	16%	
26	28.f	0.30	5.00			11	0.10	0.56	0.17	21%	
28	31.nf						0.00	0.00	0.00	0%	
29	32.f	0.30	30.00			9	0.15	0.86	0.50	26%	
30	33.fd										
32	22.f	0.05	2.00		convex	13	0.16	0.69	0.35	41%	
10A	6.f	0.20	2.00	25.00	planar	12	0.07	0.83	0.46	17%	
10S	7.f	0.20	5.00	45.00	convex	9	0.32	1.04	0.33	58%	1.702
marls	33.nf										1.857
stab area	34.nf										1.53

f: areas with open fissures, nf: areas without fissures, and fd: areas with filled fissures.

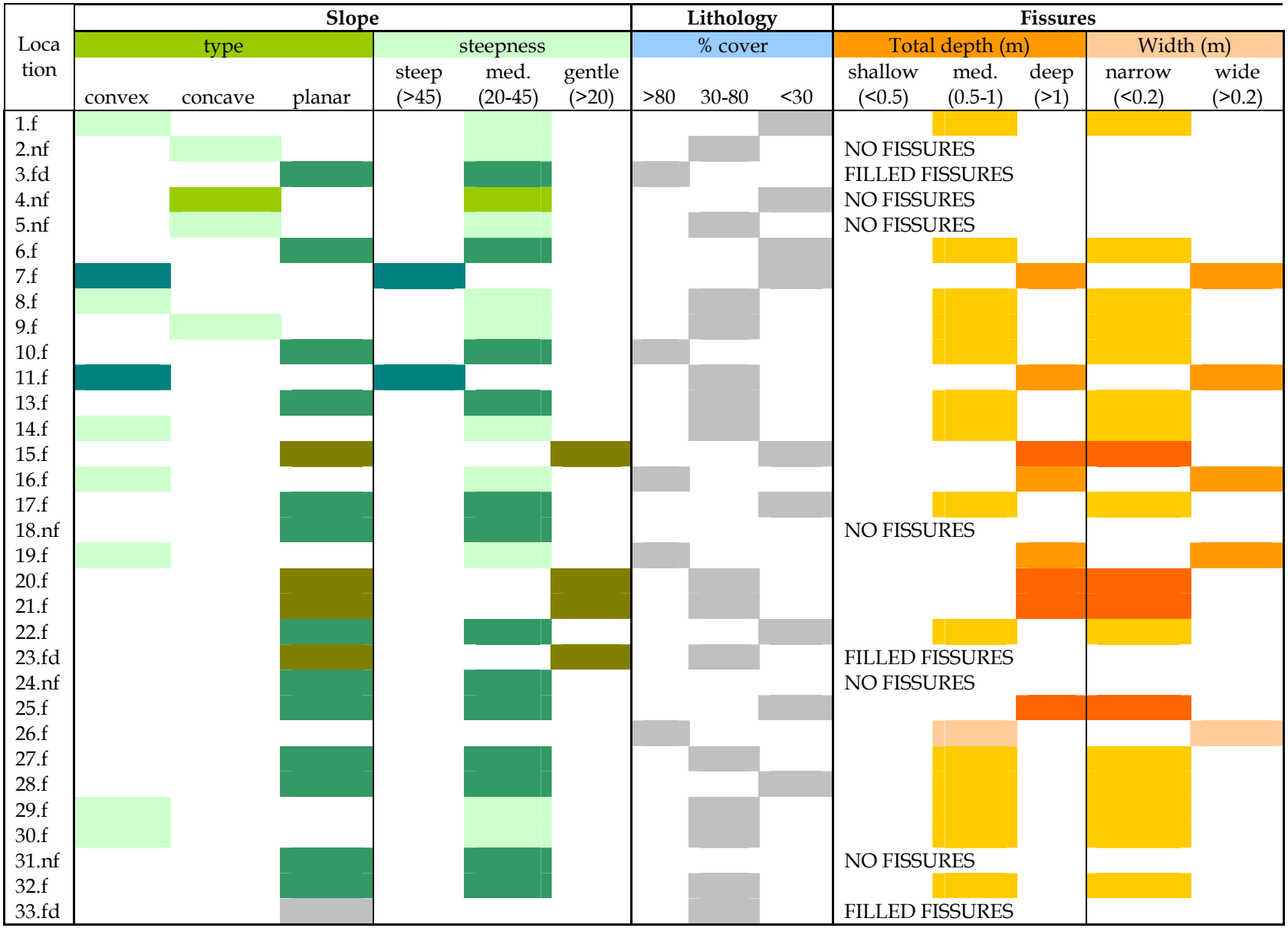
Location
Slope
type
convex
concave
planar
steepness
steep (>45)
med. (20-45)
gentle (>20)
Lithology
% cover
>80
30-80
<30
Fissures
Total depth (m)
shallow (<0.5)
med. (0.5-1)
deep (>1)
Width (m)
narrow (<0.2)
wide (>0.2)
1.f
2.nf
3.fd
4.nf
5.nf
6.f
7.f
8.f
9.f
10.f
11.f
13.f
14.f
15.f
16.f
17.f
18.nf
19.f
20.f
21.f
22.f
23.fd
24.nf
25.f
26.f
27.f
28.f
29.f
30.f
31.nf
32.f
33.fd
NO FISSURES
FILLED FISSURES
NO FISSURES
NO FISSURES
NO FISSURES
FILLED FISSURES
NO FISSURES
NO FISSURES

Appendix III. Pictures

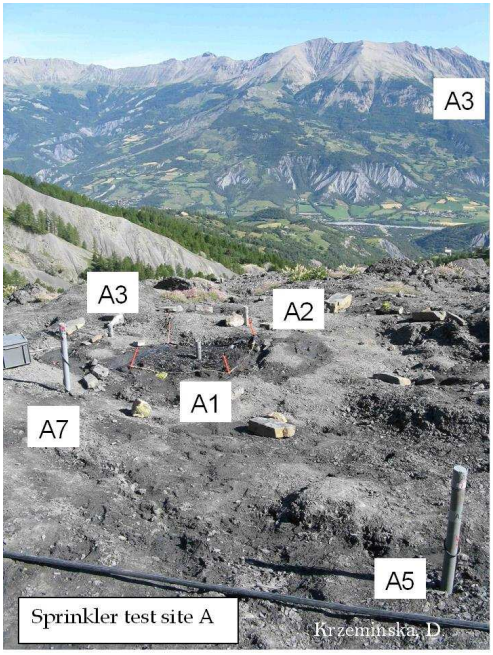

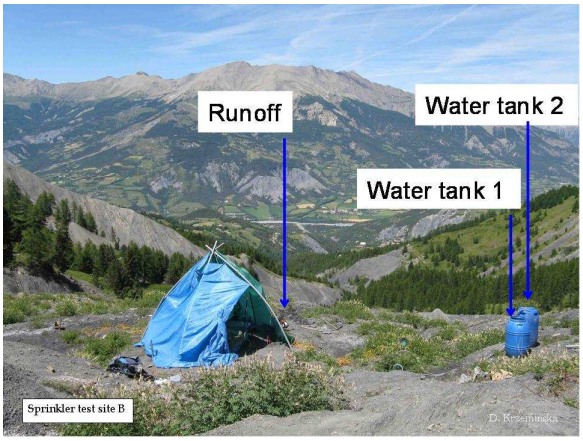

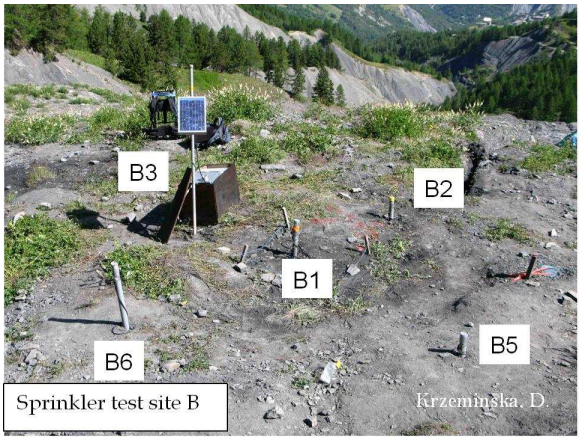

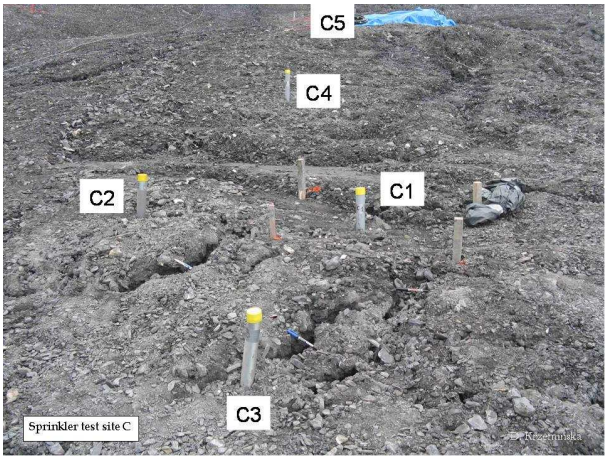


Crown, deep & wide fissures
A. Arevalo


Soil material upper part


Infiltration test in fissures
A. Arevalo


Infiltration test in matrix
A. Arevalo


Storage of rainfall
A. Arevalo


Storage of snow
A. Arevalo


Quatrocopter - UAV
A. Arevalo

Appendix IV. Soil moisture measurements

Plot A – Second day

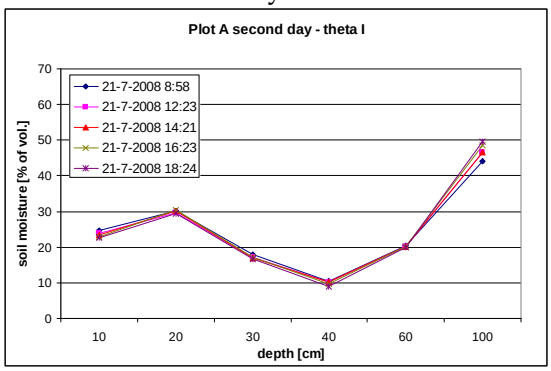

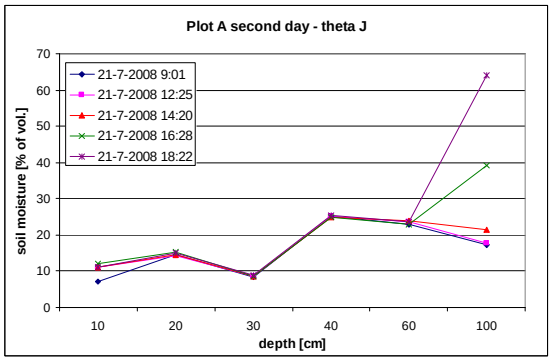

Plot C – First day

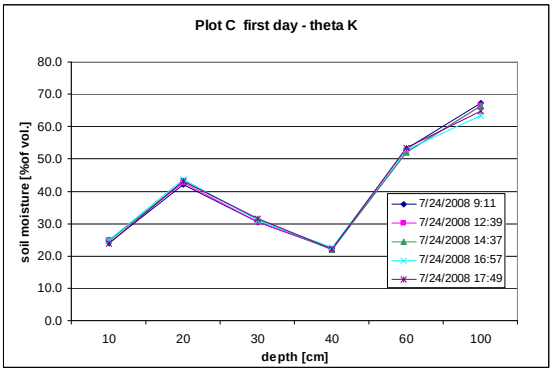

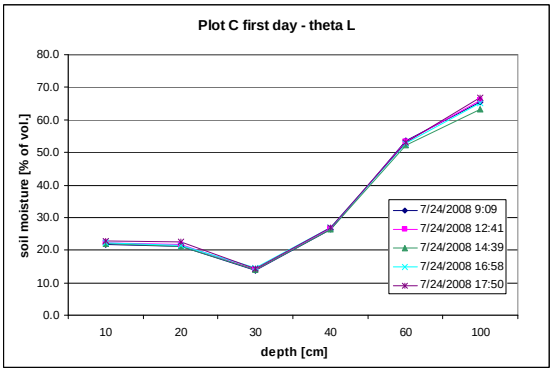

Appendix V. Sprinkler test calculations – Plot C

Water balance calculation - Plot C Day 1

DATA		
Infiltrated rain	0.364	m3
ho	1838.82	masl
h t=end+15 min	1839.06	masl
h t=end	1839.11	masl
Soil surface	1839.30	masl
Ks	3.9	m/day
Range porosity	0.38 - 0.40	[-]
Soil moisture conter	0.25	[-]
Vol moisture conten	0.0737	m3

FIXING PARAMETERS		
Porosity	0.4	[-]
Saturated area	1	m2
Sy1	0.20	[-]
Sy2	0.14	

RESULTS		
STAT cumS t=end	0.0442	m3
DYN cumS t=end	0.0479	m3
Error	0.08	%
STAT cumS t=end-	0.0979	m3
∑dS/dt	0.0157	m3
∑Qout	-0.3484	m3

$$V_{rel} = BS \frac{\Delta \phi}{\Delta t}$$

TIME	water level [masl]	RELATIVE TIME (min)	D GWL (mm)	RAINFALL [mm]	Exfiltrat (m3/3min)	Q_down from -dh/dt (m3/3min)	Q_rise from avg -dh/dt (m3/3min)	DS/Dt (m3/3min)	Accum S (m3)
7/24/08 9:01	1838.819	0:00:00	219.35						
7/24/08 10:58	1838.726	1:12:00	216.35			0.0000		0.0000	0.0000
7/24/08 11:01	1838.728	1:15:00	216.35	5.01		0.0000		0.0050	0.0050
7/24/08 11:04	1838.730	1:18:00	216.35	5.01		0.0000		0.0050	0.0100
7/24/08 11:07	1838.817	1:21:00	217.29	5.01		0.0000	0.0000	0.0050	0.0150
7/24/08 11:10	1838.924	1:24:00	324.38	5.01		0.0000	0.0000	0.0050	0.0200
7/24/08 11:13	1839.020	1:27:00	420.26	5.01		0.0000	0.0000	0.0050	0.0251
7/24/08 11:16	1839.085	1:30:00	485.50			0.0000	0.0000	0.0000	0.0251
7/24/08 11:19	1839.071	1:33:00	471.18			-0.0029	0.0000	-0.0029	0.0222
7/24/08 11:22	1839.063	1:36:00	463.05			-0.0016		-0.0016	0.0206
7/24/08 11:25	1839.058	1:39:00	457.95			-0.0010		-0.0010	0.0195
7/24/08 11:28	1839.018	1:42:00	418.20			-0.0079		-0.0079	0.0116
7/24/08 11:31	1839.043	1:45:00	442.67	5.47		0.0000	-0.0034	0.0021	0.0137
7/24/08 11:34	1839.095	1:48:00	494.68	5.47		0.0000	-0.0034	0.0021	0.0158
7/24/08 11:37	1839.108	1:51:00	507.91	5.47		0.0000	-0.0034	0.0021	0.0179
7/24/08 11:40	1839.109	1:54:00	508.91	5.47		0.0000	-0.0034	0.0021	0.0200
7/24/08 11:43	1839.104	1:57:00	503.85	5.47		-0.0010		0.0045	0.0245
7/24/08 11:46	1839.105	2:00:00	504.85			0.0000		0.0000	0.0245
7/24/08 11:49	1839.071	2:03:00	471.18			-0.0067		-0.0067	0.0177
7/24/08 11:52	1839.063	2:06:00	463.05			-0.0016		-0.0016	0.0161

TIME	water level [masl]	RELATIVE TIME (min)	D GWL (mm)	RAINFALL [mm]	Exfiltrat (m3/3min)	Q_down from -dh/dt (m3/3min)	Q_rise from avg -dh/dt (m3/3min)	DS/Dt (m3/3min)	Accum S (m3)
7/24/08 11:55	1839.058	2:09:00	457.95			-0.0010		-0.0010	0.0151
7/24/08 11:58	1839.018	2:12:00	418.20			-0.0079		-0.0079	0.0071
7/24/08 12:01	1839.063	2:15:00	463.05	5.12		0.0000	-0.0021	0.0030	0.0102
7/24/08 12:04	1839.110	2:18:00	509.91	5.12		0.0000	-0.0021	0.0030	0.0132
7/24/08 12:07	1839.114	2:21:00	513.99	5.12		0.0000	-0.0021	0.0030	0.0163
7/24/08 12:10	1839.109	2:24:00	508.91	5.12		-0.0010		0.0041	0.0204
7/24/08 12:13	1839.105	2:27:00	504.85	5.12		-0.0008		0.0043	0.0247
7/24/08 12:16	1839.098	2:30:00	497.74			-0.0014		-0.0014	0.0232
7/24/08 12:19	1839.078	2:33:00	478.34			-0.0039		-0.0039	0.0194
7/24/08 12:22	1839.064	2:36:00	464.07			-0.0029		-0.0029	0.0165
7/24/08 12:25	1839.060	2:39:00	459.97			-0.0008		-0.0008	0.0157
7/24/08 12:28	1839.063	2:42:00	463.05			0.0000	-0.0018	-0.0018	0.0139
7/24/08 12:31	1839.059	2:45:00	458.95	4.92	-0.0035	-0.0008	-0.0018	0.0023	0.0162
7/24/08 12:34	1839.100	2:48:00	499.78	4.92	-0.0035	0.0000	-0.0018	0.0031	0.0193
7/24/08 12:37	1839.104	2:51:00	503.83	4.92	-0.0035	0.0000	-0.0018	0.0031	0.0224
7/24/08 12:40	1839.101	2:54:00	500.80	4.92	-0.0035	-0.0006	-0.0018	0.0025	0.0249
7/24/08 12:43	1839.106	2:57:00	505.87	4.92	-0.0035	0.0000	-0.0018	0.0031	0.0281
7/24/08 12:46	1839.109	3:00:00	508.91			0.0000	-0.0018	-0.0018	0.0263
7/24/08 12:49	1839.105	3:03:00	504.85			-0.0008		-0.0008	0.0255
7/24/08 12:52	1839.098	3:06:00	497.74			-0.0014		-0.0014	0.0240
7/24/08 12:55	1839.078	3:09:00	478.34			-0.0039		-0.0039	0.0201
7/24/08 12:58	1839.064	3:12:00	464.07			-0.0029		-0.0029	0.0173
7/24/08 13:01	1839.060	3:15:00	459.97	5.08	-0.0035	-0.0008		0.0043	0.0216
7/24/08 13:04	1839.098	3:18:00	497.74	5.08	-0.0035	0.0000	-0.0015	0.0036	0.0251
7/24/08 13:07	1839.108	3:21:00	507.91	5.08	-0.0035	0.0000	-0.0015	0.0036	0.0287
7/24/08 13:10	1839.101	3:24:00	500.80	5.08	-0.0035	-0.0014	-0.0015	0.0021	0.0308
7/24/08 13:13	1839.108	3:27:00	507.91	5.08	-0.0035	0.0000	-0.0015	0.0036	0.0343
7/24/08 13:16	1839.095	3:30:00	494.66			-0.0027		-0.0027	0.0317
7/24/08 13:19	1839.076	3:33:00	476.26			-0.0037		-0.0037	0.0280
7/24/08 13:22	1839.064	3:36:00	464.07			-0.0024		-0.0024	0.0256
7/24/08 13:25	1839.065	3:39:00	465.09			0.0000	-0.0029	-0.0029	0.0226
7/24/08 13:28	1839.066	3:42:00	466.07			0.0000	-0.0029	-0.0029	0.0197
7/24/08 13:31	1839.074	3:45:00	474.26	4.96	-0.0032	0.0000	-0.0029	0.0020	0.0218
7/24/08 13:34	1839.106	3:48:00	505.83	4.96	-0.0032	0.0000	-0.0029	0.0020	0.0238

TIME	water level [masl]	RELATIVE TIME (min)	D GWL (mm)	RAINFALL [mm]	Exfiltrat (m3/3min)	Q_down from -dh/dt (m3/3min)	Q_rise from avg -dh/dt (m3/3min)	DS/Dt (m3/3min)	Accum S (m3)
7/24/08 13:37	1839.105	3:51:00	504.85	4.96	-0.0032	-0.0002	-0.0029	0.0018	0.0256
7/24/08 13:40	1839.108	3:54:00	507.87	4.96	-0.0032	0.0000	-0.0029	0.0020	0.0277
7/24/08 13:43	1839.095	3:57:00	494.66	4.96	-0.0032	-0.0026		0.0023	0.0300
7/24/08 13:46	1839.076	4:00:00	476.26			-0.0037		-0.0037	0.0263
7/24/08 13:49	1839.064	4:03:00	464.07			-0.0024		-0.0024	0.0239
7/24/08 13:52	1839.065	4:06:00	465.09			0.0000	-0.0029	-0.0029	0.0209
7/24/08 13:55	1839.066	4:09:00	466.07			0.0000	-0.0029	-0.0029	0.0180
7/24/08 13:58	1839.055	4:12:00	454.85			-0.0022	-0.0029	-0.0052	0.0129
7/24/08 14:01	1839.063	4:15:00	463.01	4.86	-0.0034	0.0000	-0.0029	0.0019	0.0148
7/24/08 14:04	1839.105	4:18:00	504.78	4.86	-0.0034	0.0000	-0.0029	0.0019	0.0167
7/24/08 14:07	1839.109	4:21:00	508.85	4.86	-0.0034	0.0000	-0.0029	0.0019	0.0187
7/24/08 14:10	1839.110	4:24:00	509.85	4.86	-0.0034	0.0000	-0.0029	0.0019	0.0206
7/24/08 14:13	1839.111	4:27:00	510.91	4.86	-0.0034	0.0000	-0.0029	0.0019	0.0226
7/24/08 14:16	1839.099	4:30:00	498.70			-0.0024		-0.0024	0.0201
7/24/08 14:19	1839.082	4:33:00	482.34			-0.0033		-0.0033	0.0168
7/24/08 14:22	1839.073	4:36:00	473.14			-0.0018		-0.0018	0.0150
7/24/08 14:25	1839.066	4:39:00	466.07	5.19	-0.0044	-0.0014		0.0038	0.0188
7/24/08 14:28	1839.090	4:42:00	490.48	5.19	-0.0044	0.0000	-0.0022	0.0029	0.0217
7/24/08 14:31	1839.108	4:45:00	507.85	5.19	-0.0044	0.0000	-0.0022	0.0029	0.0247
7/24/08 14:34	1839.105	4:48:00	504.80	5.19	-0.0044	-0.0006	-0.0022	0.0023	0.0270
7/24/08 14:37	1839.104	4:51:00	503.80	5.19	-0.0044	-0.0002	-0.0022	0.0027	0.0298
7/24/08 14:40	1839.110	4:54:00	509.85			0.0000	-0.0022	-0.0022	0.0275
7/24/08 14:43	1839.099	4:57:00	498.70			-0.0022		-0.0022	0.0253
7/24/08 14:46	1839.082	5:00:00	482.34			-0.0033		-0.0033	0.0220
7/24/08 14:49	1839.073	5:03:00	473.14			-0.0018		-0.0018	0.0202
7/24/08 14:52	1839.066	5:06:00	466.07			-0.0014		-0.0014	0.0188
7/24/08 14:55	1839.060	5:09:00	459.93			-0.0012		-0.0012	0.0175
7/24/08 14:58	1839.060	5:12:00	459.93			0.0000	-0.0020	-0.0020	0.0155
7/24/08 15:01	1839.077	5:15:00	477.20	5.22	-0.0034	0.0000	-0.0020	0.0032	0.0188
7/24/08 15:04	1839.108	5:18:00	507.81	5.22	-0.0034	0.0000	-0.0020	0.0032	0.0220
7/24/08 15:07	1839.109	5:21:00	508.81	5.22	-0.0034	0.0000	-0.0020	0.0032	0.0252
7/24/08 15:10	1839.115	5:24:00	514.91	5.22	-0.0034	0.0000	-0.0020	0.0032	0.0284
7/24/08 15:13	1839.114	5:27:00	513.91	5.22	-0.0034	-0.0002		0.0050	0.0334
7/24/08 15:16	1839.102	5:30:00	501.70			-0.0024		-0.0024	0.0310
7/24/08 15:19	1839.084	5:33:00	484.34			-0.0035		-0.0035	0.0275
7/24/08 15:22	1839.075	5:36:00	475.14			-0.0018		-0.0018	0.0257

Plot C - day 1

Input data

Ks	0.0081	m/3min
dist eq lines	1.47	m
Width	1	m

Results

K H1	47.78061
K H2	389.0777
Sum_Darcy	0.02708
Sum_quick	0.00190

Min_square_error 1	2.808627
Min_square_error 2	13.33737

									C3		
Time	**Relative time**	**GWL (masl)**	**Heigth on ref (cm)**	**Moving average (cm)**	**Ht**	H2-graph	H1-graph	square_diff	**GWL (masl)**	**Heigth on ref (cm)**	Qdarcy_matrix (m3/3min)
7/24/08 17:16		1839.10	20.47	20.47							
7/24/08 17:43	3	1839.11	21.16	21.16	21.160	16.629	21.160	0	1838.65	-25.10	
7/24/08 17:46	6	1839.09	19.02	19.02	19.872	16.501	19.872	0.732160598	1838.63	-27.14	0.00043
7/24/08 17:49	9	1839.08	17.79	17.79	18.663	16.374	18.663	0.756860112	1838.60	-30.40	0.00042
7/24/08 17:52	12	1839.07	16.98	16.98	17.527	16.249	17.527	0.302500434	1838.59	-31.22	0.00038
7/24/08 17:55	15	1839.06	16.47	16.47	16.460	16.124	16.460	4.58792E-05	1838.58	-31.73	0.00035
7/24/08 17:58	18	1839.06	16.47	16.47	15.459	16.000	15.459	1.017059869	1838.58	-32.04	0.00032
7/24/08 18:01	21	1839.06	15.88	15.88	15.877	15.877	15.877	0	1838.58	-32.35	0.00033
7/24/08 18:04	24	1839.05	15.17	15.52	15.755	15.755		0.054739763	1838.58	-31.94	0.00033
7/24/08 18:07	27	1839.05	15.47	15.32	15.634	15.634		0.099177155	1838.58	-32.45	0.00033
7/24/08 18:10	30	1839.06	15.67	15.57	15.514	15.514		0.003493116	1838.58	-32.35	0.00032
7/24/08 18:13	33	1839.05	15.37	15.52	15.395	15.395		0.015701644	1838.58	-32.45	0.00032
7/24/08 18:16	36	1839.05	15.27	15.32	15.277	15.277		0.001568852	1838.58	-32.35	0.00031
7/24/08 18:19	39	1839.05	14.96	15.20	15.159	15.159		0.001492787	1838.57	-32.76	0.00031
7/24/08 18:22	42	1839.05	15.27	15.16	15.043	15.043		0.014820521	1838.57	-32.55	0.00031
7/24/08 18:25	45	1839.05	15.06	15.10	14.927	14.927		0.028662638	1838.57	-32.86	0.00031
7/24/08 18:28	48	1839.05	14.76	15.03	14.813	14.813		0.046644703	1838.57	-32.96	0.00030
7/24/08 18:31	51	1839.04	14.45	14.76	14.699	14.699		0.003343542	1838.57	-32.76	0.00030
7/24/08 18:34	54	1839.04	14.45	14.55	14.586	14.586		0.00106033	1838.57	-32.96	0.00030
7/24/08 18:37	57	1839.05	14.96	14.62	14.474	14.474		0.021741843	1838.57	-33.26	0.00029
7/24/08 18:40	60	1839.05	14.76	14.72	14.363	14.363		0.130028789	1838.56	-33.67	0.00029
7/24/08 18:43	63	1839.04	14.15	14.62	14.252	14.252		0.13611805	1838.56	-33.67	0.00029
7/24/08 18:46	66	1839.05	14.55	14.49	14.143	14.143		0.117272457	1838.57	-33.47	0.00028
7/24/08 18:49	69	1839.04	14.35	14.35	14.034	14.034		0.099299792	1838.56	-33.77	0.00028
7/24/08 18:52	72	1839.04	13.64	14.18	13.926	13.926		0.064656397	1838.56	-33.87	0.00028
7/24/08 18:55	75	1839.04	14.04	14.01	13.820	13.820		0.036592387	1838.56	-34.08	0.00028
7/24/08 18:58	78	1839.04	13.84	13.84	13.713	13.713		0.016252401	1838.56	-34.08	0.00027
7/24/08 19:01	81	1839.04	14.04	13.98	13.608	13.608		0.135029492	1838.56	-34.08	0.00027
7/24/08 19:04	84	1839.04	14.14	14.01	13.504	13.504		0.255347121	1838.56	-34.28	0.00027
7/24/08 19:07	87	1839.03	13.43	13.87	13.400	13.400		0.223179283	1838.56	-34.08	0.00026
7/24/08 19:10	90	1839.03	13.13	13.57	13.297	13.297		0.073300432	1838.55	-34.79	0.00027
7/24/08 19:13	93	1839.03	13.33	13.30	13.195	13.195		0.010323637	1838.55	-34.59	0.00026